ORGANOMETALLICS

Article

pubs.acs.org/Organometallics

Radical Mechanisms in the Reaction of Organic Halides with Diiminepyridine Cobalt Complexes

Di Zhu,[†] Ilia Korobkov,[‡] and Peter H. M. Budzelaar*,[†]

[†]Department of Chemistry, University of Manitoba, Winnipeg, MB R3T 2N2, Canada

[‡]Department of Chemistry, University of Ottawa, Ottawa, ON K1N 6N5, Canada

Supporting Information

ABSTRACT: The formally Co(0) complex $LCo(N_2)$ (L = 2,6-bis(2,6-dimethylphenyliminoethyl)pyridine) can be prepared via either Na/Hg reduction of $LCoCl_2$ or hydrogenolysis of $LCoCH_2SiMe_3$. In the latter reaction, LCoH could be trapped by reaction with $N{\equiv}CC_6H_4$-4-Cl to give $LCoN{=}CHC_6H_4$-4-Cl. $LCo(N_2)$ reacts with many alkyl and aryl halides RX, including aryl chlorides, to give a mixture of LCoR and LCoX in a halogen atom abstraction mechanism. Intermediacy of free alkyl and aryl radicals is confirmed by the ring-opening of cyclopropylmethyl to crotyl, and the rearrangement of 2,4,6-^{t}Bu$_3$C$_6$H$_2$ to 3,5-^{t}Bu$_2$C$_6$H$_3$CMe$_2$CH$_2$, before binding to Co. The organocobalt species generated in this way react further with activated halides R′X (alkyl iodides; allyl and benzyl halides) to give cross-coupling products RR′ in what is most likely again a halogen abstraction mechanism. DFT studies support the proposed radical pathways for both steps. MeI couples smoothly with $LCoCH_2SiMe_3$ to give LCoI and $CH_3CH_2SiMe_3$, but the analogous reaction of ^{t}BuI leads in part to radical attack at the 3 and 4 positions of the pyridine ring to form (^{t}Bu$_2$-L)CoI and (^{t}Bu$_2$-L)CoI$_2$.

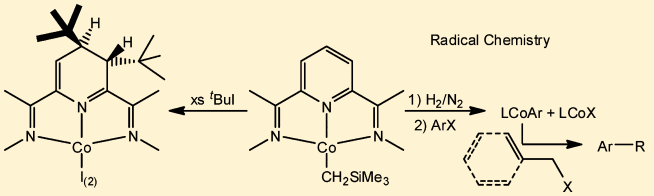

INTRODUCTION

In recent years, redox-active ligands have been intensively studied due to the unusual properties they confer on their metal complexes. Popular classes of such ligands are α-diimines,[1] α-imino-ketones,[2] and diiminepyridines (DIP);[3] the latter are especially attractive because they bind strongly to transition metals and provide considerable steric protection.

One intriguing aspect of the chemistry of redox-active ligands is the possibility of "ennobling" light transition metals,[4] making them behave more like their heavier congeners. For example, DIP complexes of iron catalyze hydrogenation and hydrosilylation,[5] in a manner more typical for the platinum metals. Whereas second- and third-row transition metals mostly exhibit low-spin states and 2*e* redox reactions, first-row transition metals tend to display high-spin states and 1*e* redox steps. However, the possibility of having transition-metal-centered unpaired electrons antiferromagnetically (AF) coupled to ligand-centered electrons opens up the possibility of having 2*e* steps where both ligand and metal are oxidized or reduced in a "coupled" fashion. On the other hand, the flexible electronic structure of complexes of redox-active ligands might also allow for new reaction modes with significant potential in synthesis and catalysis.

One of the most important redox reactions in organic synthesis is the breaking of carbon−halogen bonds. This is a key step in the catalyzed formation of C−C, C−N, and C−S bonds; in addition, C−X cleavage is required in the disposal of CFCs and similarly harmful environmental contaminants. The most common mechanisms of C−X cleavage are[6]

(a) via S_N2-like nucleophilic attack by an electron-rich metal center (mostly for alkyl halides)

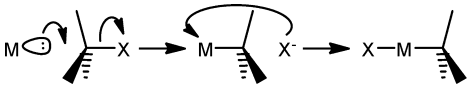

(b) via concerted addition involving a three-center transition state (mostly for aryl halides)

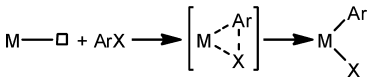

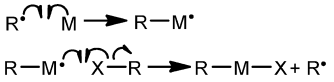

(c) via radical mechanisms (usually for activated alkyl halides)

In each of these, one typically obtains a product that has the halide and the carbon fragment attached to the same metal atom ("mononuclear oxidative addition") in an overall 2*e* oxidation step (Scheme 1, A).

Cases where the halide and the organic fragment end up on two different metal atoms in two separate 1*e* oxidation steps ("binuclear oxidative addition": Scheme 1, B) are much more rare. Most of them involve *alkyl* halides,[7−10] presumably because the Csp^3−X bond is weaker than the Csp^2−X bond as

Received: March 5, 2012
Published: May 15, 2012

   dx.doi.org/10.1021/om300182c | *Organometallics* 2012, 31, 3958−3971

Scheme 1. Schematic Representation of (A) Mononuclear and (B) Binuclear Oxidative Additions

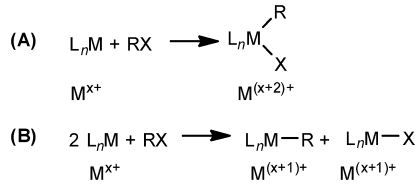

well as for steric reasons. In fact, prior to our own recent communication,[11] the only example of binuclear oxidative addition of an *aryl* halide was reported about 45 years ago,[9a] when Halpern and co-workers observed the reaction of the activated halide 2-iodopyridine with $Co(CN)_5^{3-}$ to give a mixture of $ICo(CN)_5^{3-}$ and 2-$C_5H_4NCo(CN)_5^{3-}$.

Redox-active ligands can make electrons available during metal-centered reactivity. This has been exploited, for example, by Soper in his study of Co−C and C−C bond formation at Co^{III} centers bearing amidophenolate ligands.[12] The DIP ligand has two low-lying π-acceptor orbitals and can accept up to three electrons in its extended π-system.[13] Thus, it should similarly be able to function as an electron reservoir during reactions at the metal center. Indeed, the group of Chirik observed oxidative addition of C−X and even C−O bonds to $(DIP)Fe^{(0)}$ complexes in what seems to be a traditional mononuclear oxidative addition reaction, although in many products the carbon-containing fragment had been "lost" from the metal.[7b] We decided to explore in some detail the potential of the related $(DIP)Co^{(0)}$ and $(DIP)Co^{I}$ complexes in oxidative addition reactions. For $(DIP)Co^{(0)}$, we found that surprisingly binuclear oxidative addition predominates.[11] Interestingly, the reaction works best for aryl chlorides, which are normally more difficult to activate than the corresponding bromides or iodides. We then reported that $(DIP)Co^{I}$(aryl) complexes undergo C−C coupling with benzyl halides.[14] In the present paper, we provide full details of this remarkable radical-mediated chemistry, including an exploration of the scope for C−C coupling reactions. Interestingly, the group of Chan very recently reported binuclear oxidative addition to iridium(III) porphyrin complexes,[15] so it appears that this type of reaction is not restricted to first-row transition metals.

RESULTS AND DISCUSSION

The choice of DIP ligand turned out to be critical in the present work. Most reactions have been carried out with the 2,6-$Me_2C_6H_3$-substituted ligand **1** (Scheme 2). In several cases,

Scheme 2. DIP Ligands Used in This Work

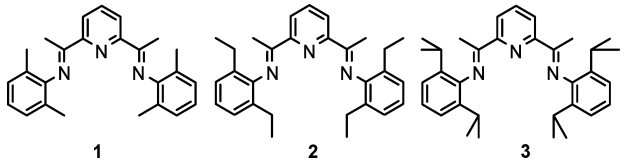

the analogous but more sterically hindered 2,6-$Et_2C_6H_3$ (**2**) and 2,6-$^i Pr_2C_6H_3$ (**3**) ligands were also tested. Unless otherwise stated, reactions mentioned in the text refer to ligand **1**.

Generation of (1)Co(N$_2$). The starting material (**1**)Co(N_2) for this study can be generated via reduction of (**1**)$CoCl_2$ with Na/Hg as described by Chirik.[16] However, we found it more convenient to generate the same species via reaction of (**1**)CoR (R = CH_2SiMe_3) in THF or benzene with a mixture of H_2 and N_2.[11] Formation of (**1**)Co(N_2) from (**1**)$CoCl_2$ and Na/Hg likely involves straightforward reduction and—at some stage—capture of a dinitrogen molecule. In contrast, the mechanism by which (**1**)Co(N_2) forms from (**1**)CoR and H_2/N_2 seems less obvious. (**3**)CoR reacts quickly with H_2 to give (**3**)CoH, which is fairly stable at room temperature and is efficient at catalyzing olefin hydrogenation,[17] a reaction that likely involves hydrogenolysis of (**3**)Co(alkyl) intermediates. Thus, one would expect treatment of (**1**)CoR with H_2 to initially produce (**1**)CoH. This hydride appears to be much less stable than (**3**)CoH,[17b] and we have never directly observed it in ^{1}H NMR spectra. However, a hydride intermediate could be trapped (Scheme 3) by treating (**1**)CoR with H_2 in the presence of

Scheme 3. Trapping of (1)CoH with PhC≡CPh and 4-N≡CC_6H_4Cl

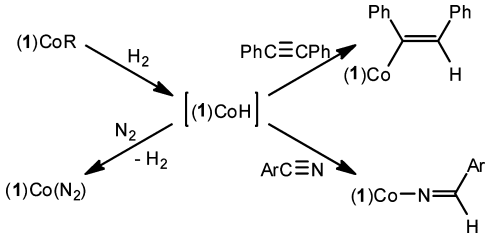

PhC≡CPh [to give (**1**)CoC(Ph)=CHPh] or 4-N≡CC_6H_4Cl [to give (**1**)CoN=CHC_6H_4Cl].

Both species were easily identified by ^{1}H NMR spectroscopy. The former could not be obtained pure but always contained either some unreacted (**1**)CoR or (**1**)$CoCH(Ph)CH_2Ph$[18] resulting from over-reduction. However, ketimide complex (**1**)CoN=CHC_6H_4Cl could be isolated and characterized by single-crystal X-ray diffraction. The structure (Figure 1) shows the square-planar Co coordination environment typical of DIP Co^{I} complexes, and a near-linear Co−N=C arrangement suggesting considerable ionic character in the Co−N bond.[19] The N4−C41−C42 angle of 124.3(6)° leaves little doubt that this is a ketimide rather than a nitrile complex; in addition, the *H*C=N resonance is prominently visible in the ^{1}H NMR spectrum at 9.62 ppm (Figure S6).

The above results strongly suggest that the initial product formed from (**1**)CoR and H_2 is (**1**)CoH or possibly (**1**)Co(H)(N_2). However, the route via which this transforms into (**1**)Co(N_2) is not clear at present. Steric hindrance appears to slow formation of the N_2 complex, since conversion of (**2**)CoH to (**2**)Co(N_2) takes about 30 min, while (**3**)CoH is stable for a day or more at room temperature. This may be taken as an indication for bimolecular elimination of H_2, e.g., via the path shown in Scheme 4. Steric hindrance would obviously slow the intermolecular H transfer step. Preliminary DFT calculations on strongly simplified models support easy transfer of hydrogen from LCo(N_2)(H) to LCoH, but accurate calculations of the complete disproportionation path for the real ligands **1**−**3** are currently not feasible.

Cleavage of C−X Bonds by LCo(N$_2$) Complexes. Many alkyl and aryl chlorides, bromides, and iodides react smoothly with green (**1**)Co(N_2) to give a purple mixture of (**1**)CoR and (**1**)CoX. While the idealized stoichiometry for this reaction would be eq 1, we typically obtained the products in a ratio (**1**)CoR:(**1**)CoX < 1:1, as detailed below.[11]

$$2LCo(N_2) + ArX \rightarrow LCoAr + LCoX + 2N_2 \quad (1)$$

dx.doi.org/10.1021/om300182c | *Organometallics* 2012, 31, 3958−3971

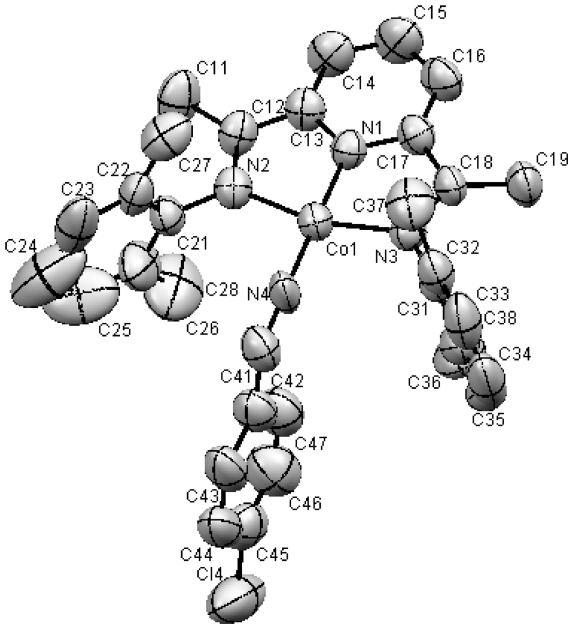

Figure 1. X-ray structure of (**1**)CoN=CHC$_6$H$_4$Cl (thermal ellipsoids drawn at 30% probability, hydrogen atoms omitted for clarity). Selected bond distances (Å) and angles (deg): Co(1)–N(1): 1.804(4); Co(1)–N(2): 1.896(4); Co(1)–N(3): 1.899(4); Co(1)–N(4): 1.726(4); C(12)–N(2): 1.336(6); C(12)–C(13): 1.423(7); C(18)–N(3): 1.330(6); C(17)–C(18): 1.453(7); N(1)– Co(1)–N(2): 81.46(17); N(4)–Co(1)–N(2): 98.79(19); N(4)–Co(1)–N(1): 178.1 (2); C(41)–N(4)–Co(1): 169.9(5); N(4)–C(41)–C(42): 124.3(6); N(2)–Co(1)–N(3): 162.9(17); C(18)–N(3)–Co(1): 116.8(3); C(12)–N(2)–Co(1): 116.2 (3).

Scheme 4. Possible Path for Reaction of (1)CoR with H_2/N_2 to Produce (1)Co(N_2)

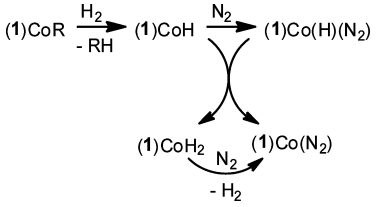

These reactions can easily be followed by ^{1}H NMR because Co^I complexes LCoZ (Z = H, alkyl, aryl, or halide) have a characteristic pyridine H4 resonance in the range 8.0–11.0 ppm, which is rather sensitive to the nature of the group Z.[17b,20] The separation of these characteristic triplets is nearly always good enough to allow reliable, quantitative determination of the relative amounts of LCoR and LCoX products. However, the resonances of several unreacted halides are obscured by other signals, since the spectra are rather crowded in both the aliphatic and aromatic regions, so the complete stoichiometry could not be established in all cases. We selected 4-ClC$_6$H$_4$CF$_3$ (which can also be observed by ^{19}F NMR) for a more complete evaluation of the influence of reaction conditions and ligand variation. Ligand effects are summarized in Table 1. The reaction of (**1**)Co(N_2) with this aryl chloride is fast (complete within 10 s). Byproducts detected in this reaction are ArH (about 10% relative to (**1**)CoCl) and Ar$_2$ (about 6%); for reactions carried out in benzene-d_6, no ArD or ArC$_6$D$_5$ could be detected by GC/MS. The reaction of (**2**)Co(N_2) is somewhat slower (~30 s), while the reaction of (**3**)Co(N_2) is much slower (hours). Interestingly, also the yield of LCoAr (relative to LCoCl) decreases in the order **1** > **2** > **3**. For

Table 1. Influence of Ligand on C–Cl Cleavage of 4-ClC$_6$H$_4$CF$_3$ by LCo(N_2)[a]

ligand	LCoAr/LCoCl	completion time[b]
1	0.77	<10 s
2	0.43	30 s
3	0.22[c]	hours

[a]LCo(N_2) (27 μmol) in around 0.4 mL of benzene-d_6, 4-ClC$_6$H$_4$CF$_3$ (3.3 μL, 27 μmol) added, reaction monitored by ^{1}H NMR. [b]Qualitative indication. [c](**3**)Co(N_2) prepared via Na/Hg reduction of (**3**)CoCl$_2$.[16]

ligand **3**, apart from (**3**)CoAr and (**3**)CoCl, a small but significant quantity of (**3**)CoH was also detected; the source of the hydride has so far remained elusive.[21]

The "oxidative addition" is slower in THF-d_8 than in C$_6$D$_6$, probably because of the stronger donor properties of the former solvent. However, neither the choice of solvent nor the concentrations of cobalt complex and aryl chloride affected the final LCoAr:LCoCl product ratio. Since ligand **1** produced the highest yield of LCoAr product, we concentrated on this ligand for further exploration of the scope of the reaction.

Table 2 summarizes the results obtained with a range of alkyl and aryl halides. The reaction product is a mixture of (**1**)CoR and (**1**)CoX, which have similar solubilities and could in most cases not be completely separated, making it impossible to obtain satisfactory elemental analyses for the new complexes (**1**)CoR. The observation in most cases of a product ratio (**1**)CoR:(**1**)CoX substantially smaller than 1 indicates some organic groups must be "lost" along the way, but we could not ascertain the fate of these groups. For 4-ClC$_6$H$_4$CF$_3$, we observed about 8% of C$_6$H$_5$CF$_3$ relative to (**1**)CoC$_6$H$_4$-4-CF$_3$ by ^{19}F NMR and could detect some (C$_6$H$_4$CF$_3$)$_2$ by GC/MS. The former could be due to hydrogen abstraction from solvent or ligand; the latter arises most likely from aryl radical dimerization. Yields in Table 2 have been calculated assuming quantitative formation of (**1**)Co(N_2) from its (**1**)CoCH$_2$SiMe$_3$ precursor, the idealized stoichiometry of eq 1,[22] and the absence of other reactions consuming ArX; the latter assumption is probably not valid for several *alkyl* halides.

From the data in the table, a few trends are clear: rates increase in the order Cl < Br < I; activated alkyls (allyl, benzyl) are more reactive; aryl halides bearing electron-withdrawing substituents react faster; and the yield of (**1**)CoAr products is largest for chlorides.

In most cases, the organocobalt product formed corresponds to the organic halide used, but there are a few exceptions: ^{i}BuBr, ^{t}BuCl, and ^{t}BuI (entries 16, 19, and 18) all give (**1**)Co^{i}Bu, although in different yields. For the latter two substrates, this is most likely due to "chain walking" of initially formed (**1**)Co^{t}Bu.[17] Similarly, ^{i}PrCl gave (**1**)Co^{n}Pr. We previously reported that (**3**)CoH adds to internal olefins to give terminal alkyls, also via chain walking.[17a]

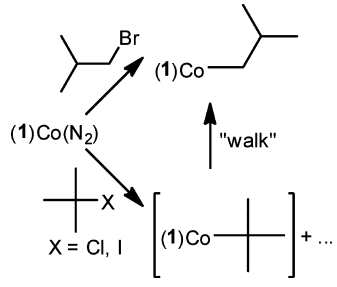

In contrast to ^{t}BuI, AdI (entry 20) did not produce *any* identifiable organocobalt complex; the only recognizable product was (**1**)CoI.

dx.doi.org/10.1021/om300182c | *Organometallics* 2012, 31, 3958–3971

Table 2. Reaction of (1)Co(N$_2$) with Organic Halides[a,b]

entry	halide RX	(1)CoR/(1)CoX[c]	yield (1)CoR, %	rxn time[d]
1	PhBr	0.25	n.d.[m]	1 min
2	PhCl	0.59	n.d.[m]	hours
3	2,4,6-^{t}Bu$_3$C$_6$H$_2$Br	0.27[e]	29	seconds
4	2,6-Me$_2$C$_6$H$_3$Cl	~0	n.d.[m]	days
5	*p*-MeCOC$_6$H$_4$Cl	0.91	71	30 min
6	*p*-CF$_3$C$_6$H$_4$Cl	0.77	89	seconds
7	*p*-ClC$_6$H$_4$Cl	0.59	48	seconds
8	*p*-MeC$_6$H$_4$Cl	0.59	38	hours
9	2,6-Cl$_2$C$_5$H$_3$N	1.0	88	seconds
10	*n*-C$_8$H$_{17}$F	n.r.		
11	(*n*-C$_6$F$_{13}$)CH=CH$_2$	0.50	25	minutes
12	CH$_2$=CHCH$_2$Cl	1.0	88	seconds
13	(cy-C$_3$H$_5$)CH$_2$Cl	0.54[f]	48	seconds
14	Br(CH$_2$)$_4$CH=CH$_2$	0.40[g]	35	seconds
15	MeI	0.71[h]	n.d.[m]	seconds
16	^{i}BuBr	0.48[i]	44	seconds
17	^{i}PrCl	0.20[j]	n.d.[m]	minutes
18	^{t}BuI	0.17[i,k]	n.d.[m]	seconds
19	^{t}BuCl	0.08[i]	8	minutes
20	AdI	~0[l]	~0	seconds

[a]Reaction conditions: (1)Co(N$_2$) generated from (1)CoCH$_2$SiMe$_3$ (27 μmol) and H$_2$ (2.0 mL) in 0.4 mL of C$_6$D$_6$; combined with ArX (27 μmol) or RX (14 μmol). [b]Entries 1–11 and 15 were already reported in our communication.[11] [c]From ^{1}H NMR, pyridine H4 peaks; estimated error margin ≈ 5%. [d]Qualitative indication. [e]Organocobalt product: R = CH$_2$CMe$_2$-3,5-^{t}Bu$_2$C$_6$H$_3$ [f]Organocobalt product: R = π-CH$_2$CHCHMe. [g]Organocobalt product: R = primary alkyl; see SI for discussion.[26] [h]Py H4 resonances of (1)CoMe and (1)CoI overlap; ratio determined from N=CC*H*$_3$ peaks. [i]Organocobalt product: R = CH$_2$CHMe$_2$. [j]Organocobalt product: R = CH$_2$CH$_2$CH$_3$ (a second diamagnetic cobalt(I) complex was also detected but could not be identified with certainty). [k]In addition, ligand attack products were observed: (1-^{t}Bu$_2$)CoI:(1)CoI ≈ 0.16. [l]An unidentified diamagnetic cobalt(I) complex was also detected. [m]Conversion of RX (and hence yield of (1)CoR) could not be determined from ^{1}H NMR.

2,4,6-^{t}Bu$_3$C$_6$H$_2$Br (entry 3) formed (1)CoCH$_2$CMe$_2$(3,5-^{t}Bu$_2$)C$_6$H$_3$.[23] The nature of this product was verified by comparison with (1)CoCH$_2$CMe$_2$C$_6$H$_5$, independently prepared from (1)CoCl$_2$ and C$_6$H$_5$CMe$_2$CH$_2$MgCl. Formation of the alkyl likely involves rearrangement of the intermediate aryl free radical.[24]

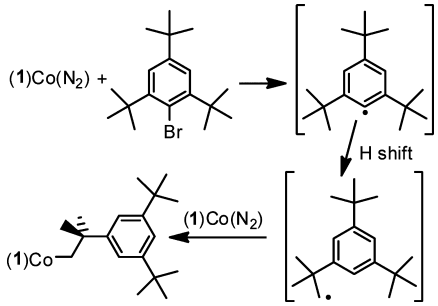

Cyclopropylmethyl chloride (entry 13) gave the η^3-crotyl complex as the only organocobalt complex. Its structure could be assigned via comparison with the independently prepared η^3-allyl complex (entry 12; *vide infra*). Opening of an intermediate cyclopropylmethyl radical[25] appears to be a reasonable explanation.

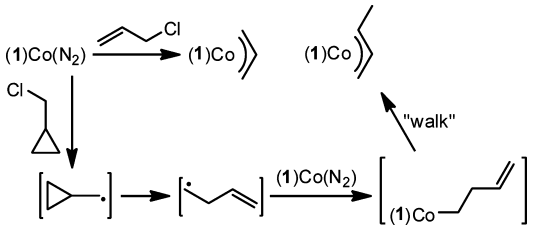

Unactivated C–F bonds do not react, but the allylic fluoride C$_6$F$_{13}$CH=CH$_2$ produced (1)Co(CH$_2$CHC$_6$F$_{12}$) in fair yield. On the basis of ^{1}H NMR parameters we believe this most likely contains a σ-bound allyl moiety (σ-CH$_2$CH=C(F)C$_5$F$_{11}$): the complex exhibits the low-field pyridine H4 resonance characteristic of square-planar LCoZ complexes, whereas the η^3-allyl and η^3-crotyl complexes mentioned above do not. Pure (1)Co(η^3-allyl) was prepared independently from (1)CoCl$_2$ and allylmagnesium chloride, and the structure was determined by single-crystal X-ray diffraction. Its molecular structure (Figure 2) is best described as a distorted square pyramid, in which the allyl group occupies an equatorial (C41) and an apical (C43) position. The C41–C42–C43 angle of 125.0(5)° is somewhat larger than usual for π-allyl complexes, but very similar to that reported for (3)Fe(η^3-allyl).[7b] In view of the dynamic behavior of the complex in solution (*vide infra*), we cannot rule out the presence of minor disorder in the allyl group, and therefore the bond lengths and angles in the allyl fragment should be treated with caution.

Solution NMR data for this π-allyl complex clearly reveal its fluxional character. At low temperature (−60 °C), the ^{1}H NMR spectrum shows different "left" and "right" sides (pyridine H3 and H5 are inequivalent) but equivalent "top" and "bottom" sides (only two Me signals for the 2,6-Me$_2$C$_6$H$_3$ groups). Also, the allyl group shows three resonances (center, *syn*, and *anti* protons) in the ratio 1:2:2. If we assume the most stable structure in solution corresponds to the solid-state one, this means that even at low temperature there is fast exchange between the two types of square pyramids (Scheme 5, reaction A). On increasing the temperature, left–right exchange becomes visible and the pyridine H3 and H5 signals broaden and coalesce, as do the two xylyl Me peaks. At somewhat higher temperature, also the allyl *syn* and *anti* signals begin to broaden and coalesce. However, fitting of the exchange-broadened spectra clearly shows that these two exchanges are distinct processes, with rates that differ by a factor of 10–100 over the range of temperatures where both can be fitted satisfactorily, the *syn*/*anti* exchange always being slowest. This suggests that the left–right exchange is an in-place rotation of the allyl group maintaining its π-coordination (Scheme 5, reaction B), while the *syn*/*anti* exchange involves interconversion of σ- and π-bound allyl groups (Scheme 5, reaction C). The activation parameters obtained from the fitted exchange rates are shown in Scheme 4 (for full details see the SI); not surprisingly, the resulting entropy of activation for σ/π exchange is somewhat larger than for in-place rotation, although the difference may not be statistically significant.

Mechanism of C–X Cleavage. As already mentioned in our preliminary communication, we believe that the actual C–X cleavage reaction follows a radical path for all or most substrates tested. On the experimental side, this is supported by the observation of radical-rearrangement products from 2,4,6-^{t}Bu$_3$C$_6$H$_2$Br and cyclopropylmethyl chloride. DFT studies also support such a mechanism. Despite extensive searches, we could not locate any transition states for conventional "side-on"

dx.doi.org/10.1021/om300182c | *Organometallics* 2012, 31, 3958–3971

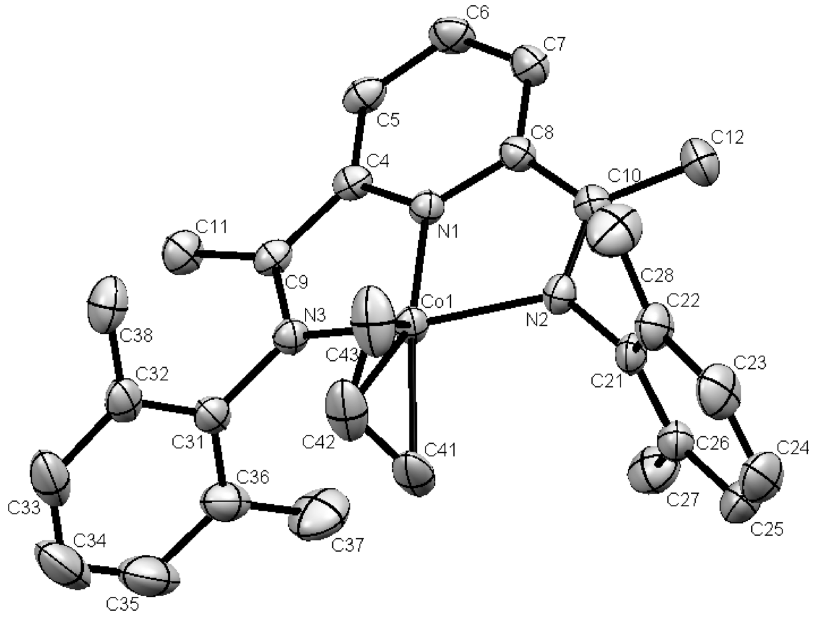

Figure 2. X-ray structure of (**1**)Co(η^3-allyl) (thermal ellipsoids drawn at 30% probability, hydrogen atoms omitted for clarity). Selected bond distances (Å) and angles (deg): Co(1)−N(1): 1.826(3); Co(1)−N(2): 1.992(3); Co(1)−N(3): 1.925(3); Co(1)−C(41): 2.070(4); Co(1)−C(42): 2.016; Co(1)−C(43): 2.131(5); C(4)−C(9): 1.414(5); N(3)−C(9): 1.338(4); N(1)−C(4): 1.378(4); N(1)−C(8): 1.368(4); C(8)−C(10): 1.425(5); N(2)−C(10): 1.320(4); C(42)−C(43): 1.346(7); C(41)−C(42): 1.381(7); N(1)−Co(1)−N(3): 80.57(12); N(1)−Co(1)−N(2): 79.14(12); N(3)−Co(1)−N(2): 152.96(12); N(1)−Co(1)−C(43): 122.20(18); N(1)−Co(1)−C(42): 153.5(2); N(1)−Co(1)−C(41): 166.76(19); C(41)−Co(1)−C(43): 70.3(2); C(43)−C(42)−C(41): 125.0(5).

Scheme 5. Fluxional Behavior of (1)Co(η^3-C_3H_5)[a]

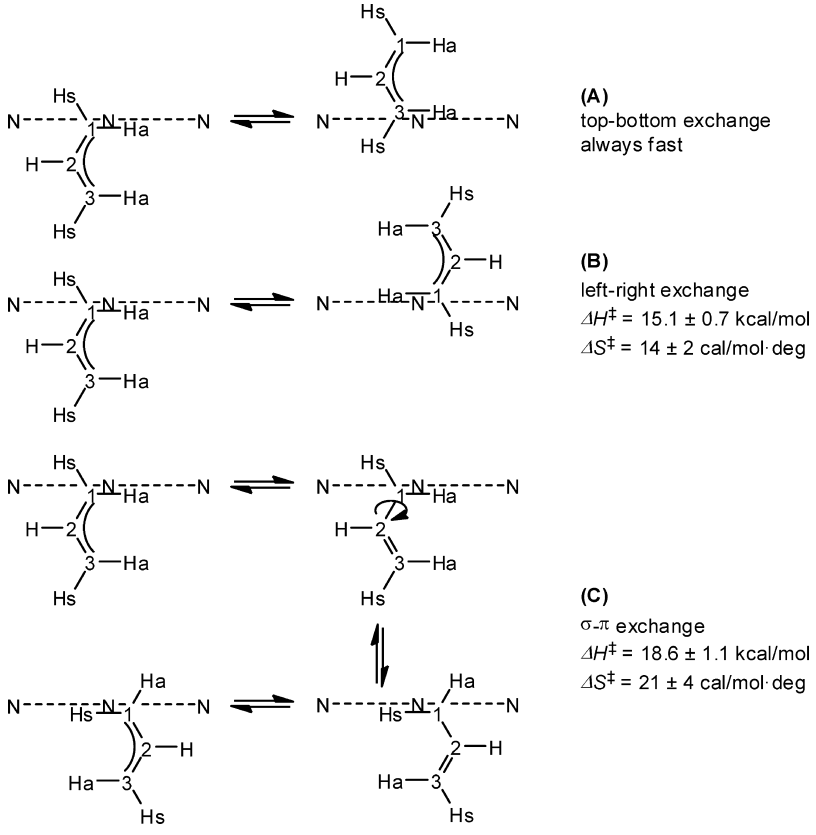

[a]Activation parameters (1σ error limits) obtained from Arrhenius plots to fitted exchange rates.

attack of Co on the C−X bond of aryl halides. All searches eventually converged to saddle points where only the halide is close to the cobalt atom, and the imaginary mode is predominantly a C−X stretch (Scheme 6).

dx.doi.org/10.1021/om300182c | *Organometallics* 2012, 31, 3958−3971

Scheme 6. Schematic Representation of Br Abstraction TS[a]

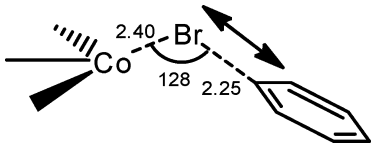

[a]Bond lengths in Å, angle in deg; the double arrow represents the imaginary mode.

Consistent with the observed relative reactivity of the various halides, the free energy barrier calculated for PhBr (19.0 kcal/mol) is substantially lower than that for PhCl (23.2 kcal/mol),[11] and the magnitude of both barriers is consistent with reactions happening around room temperature (1 min for PhBr, hours for PhCl). One possible mechanistic picture for the complete reaction is shown in Scheme 7. The

Scheme 7. Proposed Reaction Mechanism for Reaction of $LCo(N_2)$ with Aryl Halides

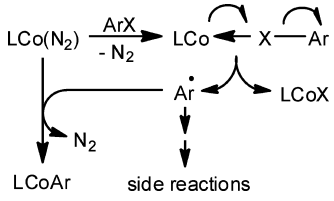

aryl halide first displaces N_2 from the metal (the retarding effect of THF, mentioned earlier, can be ascribed to competition between THF and ArX for the empty site at Co). Then, C–X cleavage results in expulsion of an aryl radical, which will independently make its way to a second Co center. Such radicals are highly reactive, and the low yield for some substrates may be due to the ease with which these radicals undergo side reactions. Also, the lower yields for bromides and iodides (compared to chlorides) might be due to the larger concentration of radicals formed, leading to a higher probability of radical combination.[27]

It is interesting to contrast this reaction mechanism with the one for addition of vinyl acetate to $(\mathbf{3})Fe(N_2)_2$, where Chirik explained formation of the "traditional" product $(\mathbf{3})Fe(C_2H_3)(OAc)$ via standard mononuclear oxidative addition.[7b] In $(\mathbf{3})Fe(N_2)_2$, the metal has the actual oxidation state +II and is intermediate-spin;[28] its two unpaired electrons each AF couple to a ligand-centered electron. In the oxidative addition, both reducing electrons come from the ligand, and the electronic structure is completely changed, with the product containing high-spin Fe^{II} and an "innocent" DIP ligand.[29] In $(\mathbf{1})Co(N_2)$, the metal is low-spin (diamagnetic) Co^{I}, with only a small amount of spin polarization at the metal (Figure 3, left); the single unpaired electron resides in a ligand π^*-orbital.[28]

The halide abstraction product $(\mathbf{1})CoX$ has low-spin Co^{II} AF coupled to a ligand-centered unpaired electron[20] (Figure 3, right). Therefore, to proceed from reactant to product one could imagine simple transfer of a single Co d electron to the aryl halide; its remaining partner could then AF couple to the ligand-centered electron to smoothly give the product. However, this is not what we find. At the transition state for C–X bond cleavage, the metal has undergone a spin-flip to *high-spin* Co^{I} (two β electrons); an amount of spin density corresponding to one α electron is spread out over both the DIP ligand and the aryl halide, apparently in the process of being transferred from one to the other (Figure 3, middle). The change in metal spin state at this point is also evident from the increase in Co–N bond lengths, by about 0.1 Å for $Co–N_{py}$ and nearly 0.2 Å for $Co–N_{im}$. Finally, the reduction in DIP ligand π^* population results in an increase of the $C_{py}–C_{im}$ bond lengths and a shortening of the C=N bonds. After the electron has been transferred and the phenyl radical ejected, at some point one of the two metal-centered unpaired electrons has to flip *and* transfer to the ligand to produce the ground state of the product LCoX. These movements and flips of electrons are summarized in Scheme 8.

Scheme 8. Movements and Flips of Electrons during Reaction of $(\mathbf{1})Co(N_2)$ with PhBr

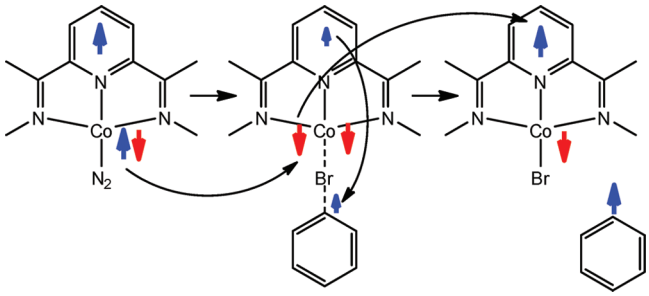

Thus, the ArX halide abstraction process appears to be more complicated than one might at first imagine, involving a

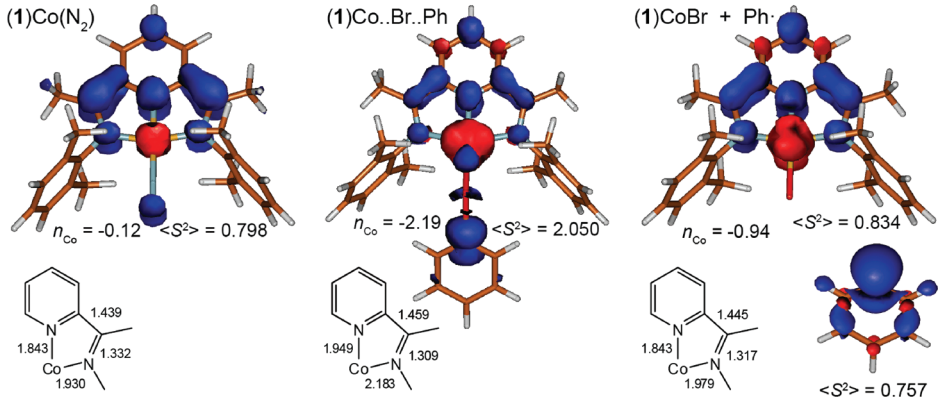

Figure 3. Spin density plots for $(\mathbf{1})Co(N_2)$, the Ph–Br cleavage transition state, and the final products $(\mathbf{1})CoBr$ and Ph·. The sign of the spin population on Co (n_{Co}) is given relative to that of density on the ligand. Bond lengths in Å.

dx.doi.org/10.1021/om300182c | *Organometallics* 2012, 31, 3958–3971

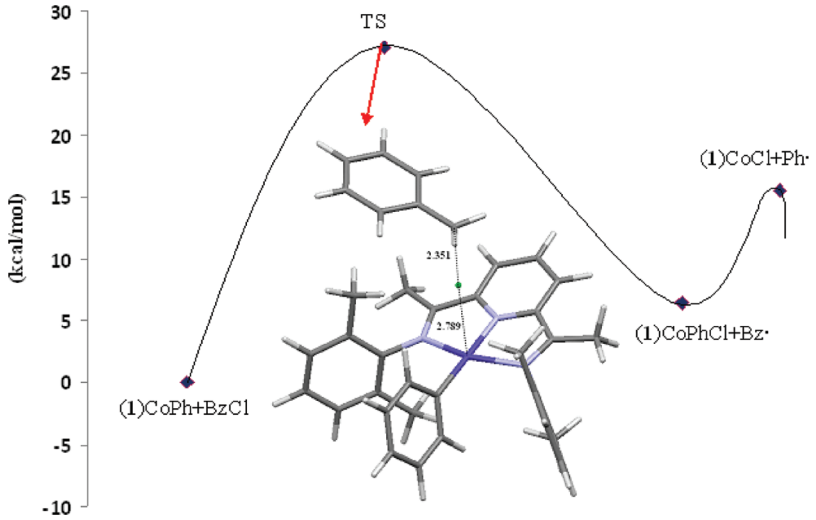

Figure 4. Free-energy profile (Δ*G*, kcal/mol, b3-lyp/TZVPP//b3-lyp/TZVP) for the reaction between (**1**)CoPh and benzyl chloride (BzCl).

temporary spin flip even though there is no obvious need for one; this is unlike, for example, the halide abstractions described by Soper,[2a] where the ligand functions as an electron reservoir and the metal (Co^{III}) appears to be truly innocent. It is not clear at present how essential these details are to the different reaction outcomes.

C−C Coupling Reactions. Since "standard" oxidative addition is so important in metal-catalyzed C−C coupling reactions, we decided to investigate whether the alkyl and aryl complexes studied here can also be used to effect C−C coupling reactions. Complexes (**1**)CoAr and (**1**)CoR were found to be much less reactive than (**1**)Co(N_2) toward organic halides; only activated halides (allyl, benzyl, or iodides) reacted at all (Table 3).[14] Complexes (**1**)CoAr bearing electron-withdrawing substituents at the Ar group are further deactivated, to the extent that, for example, complex **4** (formed from 2,6-dichloropyridine) is slower to react with benzyl chloride (BzCl) than even (**1**)CoCl.

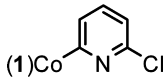

4

In most cases where reaction did occur, the major product was the heterocoupling product, but significant amounts of one or both possible homocoupling products were observed as well, indicating that also this coupling reaction most likely involves free radicals. DFT calculations support this idea: we were able to locate a transition state for abstraction of a chlorine atom from benzyl chloride by (**1**)CoPh, with a calculated activation energy of 27.1 kcal/mol (for the reaction profile, see Figure 4). The complex (**1**)Co(Ph)(Cl) formed this way should easily lose a phenyl radical, which can combine with the earlier generated benzyl radical. Some product may also be formed by a benzyl radical attacking intact (**1**)CoPh, to first form (**1**)Co(Bz)(Ph) and then eliminate PhBz; the naked (**1**)Co left this way could reduce the next benzyl chloride molecule. This C−C coupling reaction is complicated by the fact that halides (**1**)CoX, always formed together with (**1**)CoR, also react slowly with allyl and benzyl halides.

Ligand Attack with ^{t}BuI. Metal-catalyzed C−C coupling involving two sp^3 carbons tends to be more difficult than coupling involving at least one sp^2 or sp carbon. However, we find that MeI couples smoothly with (**1**)$CoCH_2SiMe_3$ to give $EtSiMe_3$. This led us to check whether our system also allows coupling involving a tertiary alkyl group, which is normally one of the more difficult couplings to achieve. Unfortunately, reaction of (**1**)$CoCH_2SiMe_3$ with ^{t}BuI did not produce any ^{t}BuCH_2SiMe_3. Instead, we obtained a mixture containing one major diamagnetic cobalt complex (with a complicated ^{1}H NMR spectrum) and one or more[30] paramagnetic complexes. A few crystals of the diamagnetic component were obtained, and refinement indicated the presence of ^{t}Bu substituents at positions 3 and 4 of the pyridine ring. However, the crystal exhibits

Table 3. Reaction of Mixtures (1)CoR/(1)CoCl with Activated Alkyl Halides R′X[a,b]

			products detected (%)[c]		
entry	R	R′X	RR′	RR	R′R′
1	*p*-$CF_3C_6H_4$	CH_2=$CHCH_2Cl$	77	23	n.o.[h]
2	C_6H_5	CH_2=$CHCH_2Cl$	84	16	n.o.[h]
3	*p*-$MeOC_6H_4$	CH_2=$CHCH_2Cl$	94	6	n.o.[h]
4	*p*-ClC_6H_4	$C_6H_5CH_2Cl$	50	n.o.	50
5	*p*-$CF_3C_6H_4$	$C_6H_5CH_2Br$	23	n.o.	77
6	C_6H_5	$C_6H_5CH_2Br$	55	39	6
7	C_6H_5	$C_6H_5CH_2Cl$	77	22	1
8	*π*-crotyl	$C_6H_5CH_2Cl$	100	n.o.	n.o.
9	CH_2SiMe_3[e]	MeI	100	n.o.	n.o.
10	*p*-MeC_6H_4[g]	MeI	93	<1	7
11	C_6H_5	C_6H_5I	n.r.		
12	C_6H_5[f]	*n*-$C_6H_{13}Br$	n.r.		
13	*p*-$CF_3C_6H_4$	^{n}BuCl	n.r.		
14	*p*-$MeOCOC_6H_4$	$C_6H_5CH_2Cl$	n.o.	n.o.	100
15	6-Cl-2-C_5H_3N	$C_6H_5CH_2Cl$	n.o.	n.o.	100
16	6-Cl-2-C_5H_3N	$C_6H_5CH_2Br$[g]	trace	n.o.	100

[a]A mixture of (**1**)CoAr + (**1**)CoCl generated from (**1**)Co(N_2) as described in Table 2, then addition of 0.5 equiv of RX relative to original ArX used. [b]Entries 1−7, 9, 15, and 16 were already reported in our mini-review.[14] [c]By GC/MS; not calibrated. [d]Calibrated against authentic samples of PhPh, PhBz, and BzBz. [e]Using separately prepared (**1**)$CoCH_2SiMe_3$ and 1.8 equiv of CH_3I; product identified by NMR and GC/MS. [f]Using separately prepared (**1**)CoPh. [g]Using 2.0 equiv of BzBr relative to (**1**)Co(N_2). [h]Any R′R′ (1,5-hexadiene) formed would have been missed due to its low boiling point.

dx.doi.org/10.1021/om300182c | *Organometallics* 2012, 31, 3958−3971

serious disorder or twinning problems, and the structure determination results cannot be taken as definitive evidence even for the connectivity of the complex (for details, see the SI). Because of these issues, we also studied the reaction of (**2**)$CoCH_2SiMe_3$ with ^{t}BuI. This produces diamagnetic and paramagnetic complexes with ^{1}H MR spectra very similar to those obtained from (**1**)$CoCH_2SiMe_3$. Again, complete separation proved impossible, but several crystallization attempts eventually produced some acceptable crystals of both components. The structures of (^{t}Bu$_2$-**2**)CoI_2 (the paramagnetic component) and (^{t}Bu$_2$-**2**)CoI (the diamagnetic component, contaminated with about 6% of cocrystallized (^{t}Bu$_2$-**2**)CoCl) are shown in Figure 5 and Figure 6,

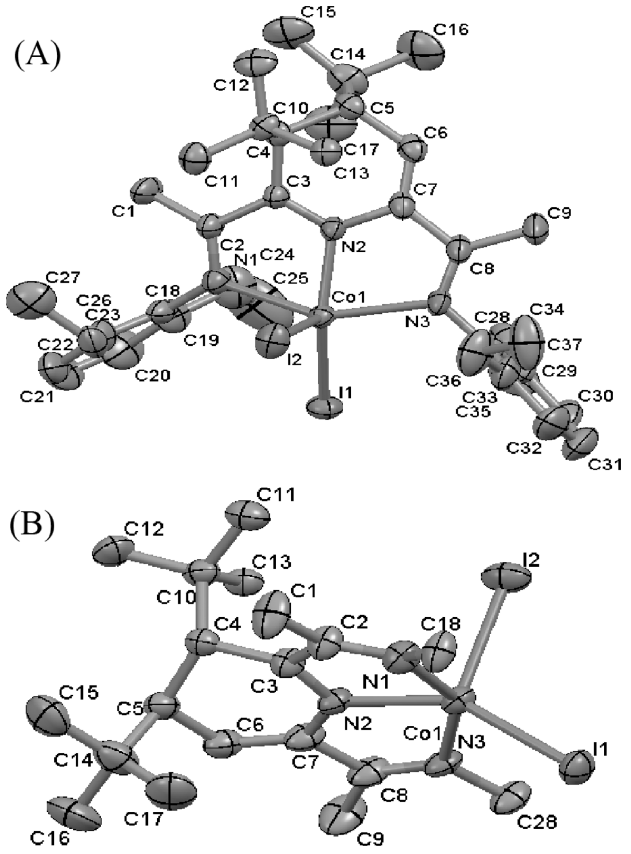

Figure 5. X-ray structure of (^{t}Bu$_2$-**2**)CoI_2 (40% thermal ellipsoids). In (B), most carbon atoms of the ligand N-aryl groups have been omitted for clarity. Selected bond distances (Å) and angles (deg): Co(1)−N(1): 2.221(3); Co(1)−N(2): 2.034(3); Co(1)−N(3): 2.213(3); C(2)−C(3): 1.501(5); N(1)−C(2): 1.281(5); C(7)−C(8): 1.472(6); N(3)−C(8): 1.280(5); N(2)−C(3): 1.279(5); C(3)−C(4): 1.510(5); C(4)−C(5): 1.542(5); C(5)−C(6): 1.512(6); C(6)−C(7): 1.334(6); N(2)−C(7): 1.400(5); N(2)−Co(1)−N(1): 73.93(11); N(2)−Co(1)−N(3): 75.78(11); N(3)−Co(1)−N(1): 147.79(12); N(2)−Co(1)−I(1): 143.28(8); N(2)−Co(1)−I(2): 104.67(8); C(7)−C(6)−C(5): 122.2(3); N(2)−C(3)−C(4): 122.3(3); C(3)−C(4)−C(5): 108.8(3); C(6)−C(5)−C(4): 110.7(3); C(10)−C(5)−C(4)−C(14): −146.3(4).

respectively. A comparison of the structures shows that the ligand in (^{t}Bu$_2$-**2**)CoI_2 is "innocent" (imine bond lengths close to 1.28 Å), whereas the ligand in (^{t}Bu$_2$-**2**)CoI appears to have accepted an electron (imine bond lengths 1.328(4) and 1.296(4) Å) in a manner very similar to Co(I) complexes of the original DIP ligand. Thus, the interruption of conjugation in the DIP skeleton caused by the two ^{t}Bu substituents does not appear to affect the electron-accepting properties of the ligand much.

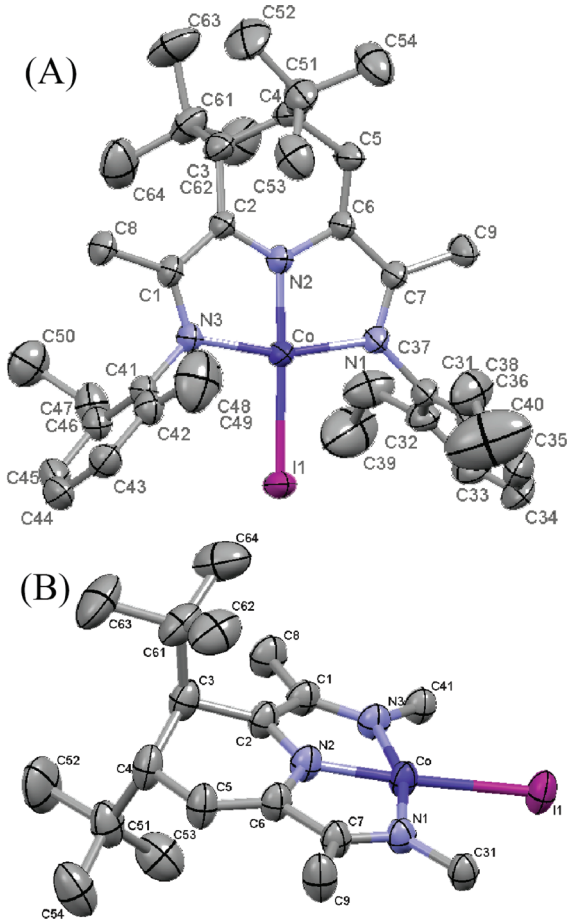

Figure 6. X-ray structure of (^{t}Bu$_2$-**2**)CoI (40% thermal ellipsoids). In (B), most carbon atoms of the ligand N-aryl groups have been omitted for clarity. Selected bond distances (Å) and angles (deg): Co(1)−I(1): 2.5170(12); Co(1)−N(1): 1.955(3); Co(1)−N(2): 1.810(3); Co(1)−N(3): 1.918(3); C(1)−C(2): 1.422(5); N(3)−C(1): 1.328(4); C(6)−C(7): 1.460(5); N(1)−C(7): 1.296(4); N(2)−C(2): 1.330(4); C(2)−C(3): 1.510(5); C(3)−C(4): 1.542(6); C(4)−C(5): 1.509(6); C(5)−C(6): 1.337(5); N(2)−C(6): 1.396(5); N(1)−Co(1)−N(2): 82.30(12); N(2)−Co(1)−N(3): 80.45(12); N(1)−Co(1)−N(3): 162.67(12); N(2)−Co(1)−I(1): 175.94(10); C(4)−C(5)−C(6): 121.0(3); N(2)−C(2)−C(3): 120.2(3); C(2)−C(3)−C(4): 110.2(3); C(3)−C(4)−C(5): 111.4(3); C(61)−C(3)−C(4)−C(51): 144.9(4).

The most reasonable mechanism for formation of the modified ligands ^{t}Bu$_2$-L is sequential attack of ^{t}Bu radicals (formed via halide abstraction) on intact LCoR and/or LCoI complexes, possibly accompanied by iodide redistribution between Co^I and Co^{II} complexes. Alkylation of DIP ligands is quite common,[31] but multiple alkylation is rare.[32] It should be noted here that the first ^{t}Bu group acts as an oxidant, changing the formally neutral ligand into a monoanionic one; the second ^{t}Bu group then acts as a reductant, so that the final ligands ^{t}Bu$_2$-L are formally neutral again. It is not clear at this point whether the initial attack occurs at carbon 3 or 4 of the pyridine ring, but since attack at C3 is extremely rare[33] initial C4 attack seems more likely. Curiously, the corresponding reaction with 1-iodoadamantane did not result in similar ring-alkylated products.

■ CONCLUSIONS

This work demonstrates the first well-defined binuclear oxidative addition reactions applicable to a variety of alkyl and aryl halides, including aryl chlorides. The required highly reactive

dx.doi.org/10.1021/om300182c | *Organometallics* 2012, 31, 3958−3971

starting material (1)Co(N_2) can be obtained via either hydrogenolysis of (1)CoCH_2SiMe_3 or reduction of (1)$CoCl_2$ in the presence of N_2. The steric properties of the ligand are important here, ligand **1** giving much better results than the more hindered variations **2** and **3**. We obtained strong indications—from both experiment and theory—that these reactions proceed via free radicals. Also, the resulting Co alkyls and aryls could be used in further C−C coupling reactions with activated alkyl halides, though not yet in a catalytic fashion. These results are significant not only in themselves, but also because they provide well-defined model systems for (presumably radical-based) C−C coupling reactions involving much less well-defined low-valent metal species, such as $CoBr_2$(2,2′-bipyridine)/Mn/pyridine, Co$(acac)_3$/PPh_3/Grignard reagent.[34] We hope that eventually our binuclear oxidative addition can be made cleaner and more efficient by generating (1)Co(N_2) *in situ* from (1)CoX, thus allowing complete conversion to (1)CoAr; the trick here will be to find a reductant that does not react with (1)CoAr (Scheme 9).

Scheme 9. Possible Route for Complete Conversion of (1)CoX to (1)CoAr

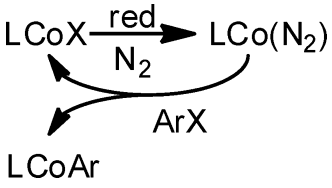

Making the C−C coupling described in the present work fully catalytic, by using a mixture of a reductant, halides RX and R′X, and a catalytic amount of (1)CoX, is likely to be difficult, and one would normally expect preferential homocoupling of the most reactive halide (this in addition to the reduction issue mentioned above). However, the price of Co (relative to, for example, Pd) is such that even a batch process involving a separate recycling step might be acceptable, provided interesting coupling products can be identified.

EXPERIMENTAL SECTION

General Considerations. All experiments were done under an argon atmosphere using standard Schlenk techniques or in a nitrogen-filled drybox. Pentane, hexane, toluene, diethyl ether, tetrahydrofuran, THF-d_8, benzene, and benzene-d_6 were distilled from sodium/benzophenone. Phenyl lithium (1.8 M in di-*n*-butyl ether) was purchased from Aldrich and used as received. Ligands **1**−**3** were prepared according to published procedures.[35,36] (1)CoCH_2SiMe_3 was prepared according to the literature procedure using (TMEDA)Co$(CH_2SiMe_3)_2$.[37] (3)-CoCH_2SiMe_3 was prepared according to the reported procedure.[38] Anhydrous chlorobenzene and anhydrous benzotrifluoride were purchased form Aldrich and used as received. Other aryl halides and alkyl halides used for oxidative additions were purchased from Aldrich or Acros, degassed, and dried over 4 Å molecular sieves in a drybox before use. Alkyl halides used in C−C coupling reactions were used as received.

^{1}H NMR, ^{13}C{H} NMR, and ^{19}F NMR spectra were recorded on a Bruker Avance 300 MHz or Bruker Avance 500 MHz spectrometers. All NMR shifts (δ, ppm) of ^{1}H NMR and ^{13}C NMR spectra were referenced to the solvent (benzene-d_6, ^{1}H NMR: C_6D_5H δ 7.16; ^{13}C NMR: C_6D_6 δ 128.0; $CDCl_3$, ^{1}H NMR: $CHCl_3$ δ 7.26; ^{13}C NMR: $CHCl_3$ δ 77.0; THF-d_8; ^{1}H NMR: OC*H*D δ 3.62; ^{13}C NMR: OCD_2 δ 68.03). Coupling constants *J* are given in Hz. Where necessary, COSY or HSQC NMR spectra were also acquired to assist ^{13}C NMR and/or ^{1}H assignments. ^{1}H peaks detected only via COSY (hence with unknown splitting patterns) are indicated by *. Data were collected at room temperature unless otherwise noted. GC/MS instrument: Varian 3800 gas chromatograph with a 30 m VF-5 ms column coupled to a Varian 320-MS operated in single quadrupole mode. KBr pellets for IR spectra were prepared in a N_2-filled drybox and measured in a Bruker Tensor27 IR instrument prepurged with nitrogen. The IR data were processed using OPUS6.5 software. Elemental analysis was done by Guelph Chemical Laboratories Ltd.

(2)CoCH_2SiMe_3. Complex (2)$CoCl_2$ (0.44 g, 0.79 mmol) was suspended in around 12 mL of dry toluene. In a N_2-filled glovebox, solid LiCH_2SiMe_3 (0.15 g, 1.59 mmol) was dissolved in 6 mL of toluene, and the resulting clear solution was slowly dropped into the above (2)$CoCl_2$ suspension over 3 h. The resulting mixture turned purple and was stirred overnight. After filtering over Celite, the purple filtrate was evaporated to dryness. The resulting residue was dissolved in toluene and layered with pentane at −35 °C over two days. Some dark solid (0.044 g) precipitated, which was determined to be (2)$CoCl_2$. The mother liquor was evaporated to dryness, and the residue was crystallized from Et_2O/pentane at −35 °C, giving 0.15 g (33%) of a dark purple solid.

^{1}H NMR (benzene-d_6, 300 MHz): δ 10.05 (1H, t, *J* 7.6, Py *H4*), 7.72 (2H, d, *J* 7.6, Py *H3*), 7.52 (2H, t, *J* 7.6, NAr *p*), 7.39 (4H, d, *J* 7.6, NAr *m*), 2.49−2.69 (8H, m, CH_2CH_3), 1.09 (12H, t, *J* 7.6, CH_2CH_3), 0.72 (2H, s, CoCH_2), −0.66 (9H, s, $SiMe_3$), −1.09 (6H, s, N=C*Me*). ^{13}C NMR (benzene-d_6, 75 MHz): δ 166.0, 157.0, 155.4, 135.6, 126.4 (NAr *p*), 126.2 (NAr *m*), 123.4 (Py *C3*), 116.3 (Py *C4*), 24.7 (CH_2CH_3), 24.0 (N=C*Me*), 13.3 (CH_2CH_3), 3.5 ($SiMe_3$). The $CoCH_2$ resonance was not observed, probably due to broadening by the quadrupolar Co. Anal. Calcd for $C_{33}H_{46}CoN_3Si$ (571.76): C, 69.32; H, 8.11; N, 7.35. Found: C, 69.59; H, 7.85; N, 7.08.

Hydrogenolysis of (2)CoCH_2SiMe_3 and Subsequent Reaction with $CF_3C_6H_4$-4-Cl. In a N_2-filled drybox, (2)CoCH_2SiMe_3 (15 mg, 26 μmol) was dissolved in 0.4 mL of benzene-d_6. Outside the drybox, 2 mL of H_2 was injected into it. The sample first turned blue-purple [5 min after the injection; at this stage, the ^{1}H NMR spectrum showed a mixture of (2)CoH and (2)Co(N_2)], then gray, and finally green (30 min after the injection of H_2). The ^{1}H NMR spectrum after 30 min showed mainly (2)Co(N_2), but a trace amount of (2)CoH was still observed. After one night, the ^{1}H NMR showed there was no (2)CoH left. The NMR sample was transferred into the drybox and flushed with nitrogen to remove the excess of hydrogen. Into this sample was injected 3.3 μL of 4-$CF_3C_6H_4Cl$ (24 μmol), and the tube was immediately shaken well to obtain good mixing. The sample turned purple in about 30 s. The ^{1}H NMR showed that there was no (2)Co(N_2) left, but unreacted 4-$CF_3C_6H_4Cl$ could still be detected; from the ratio of the pyridine H4 resonances, (2)CoC_6H_4-4-CF_3:(2)CoCl = 0.43:1.

Tentative, partial assignments for (2)CoC_6H_4-4-CF_3: ^{1}H NMR (benzene-d_6, 300 MHz): δ 10.21 (1H, br, Py *H4*), 4.77 (2H, br, CoAr *o*), −0.78 (6H, s, N=C*Me*). ^{19}F NMR (25 °C, benzene-d_6, 282 MHz): δ −61.2.

Hydrogenolysis of (3)CoCH_2SiMe_3 in the Presence of Dinitrogen. In a N_2-filled drybox, (3)CoCH_2SiMe_3 (17.1 mg, 27 μmol) was weighed into a small vial and dissolved in 0.4 mL of benzene-d_6. The resulting purple solution was transferred into an NMR tube. Outside the drybox, 2.0 mL of H_2 was injected into it. After 5 min, all (3)CoCH_2SiMe_3 had been converted into (3)CoH; no (3)Co(N_2) could be detected by ^{1}H NMR. After 1 h, some solid precipitated at the bottom of the NMR tube and ^{1}H NMR showed only (3)CoH. After 24 h, the sample had turned violet and more solid had precipitated. The ^{1}H NMR spectrum at this stage showed the presence of a small amount of (3)Co(N_2); the main complex in solution was still (3)CoH. Longer standing resulted in the precipitation of more black solids.

Reaction of (3)Co(N_2) with 4-$CF_3C_6H_4Cl$ (ref 14). In a N_2-filled drybox, (3)Co(N_2)[16] (11.8 mg, 20 μmol) was weighed and dissolved in about 0.4 mL of dry benzene-d_6; 4-$CF_3C_6H_4Cl$ (2.45 μL, 19.6 μmol) was then added. The mixture turned gray-blue. The immediately recorded ^{1}H NMR spectrum showed that the reaction was not complete [still (3)Co(N_2) visible], and three diamagnetic cobalt(I) complexes could be clearly observed: (3)CoH:(3)CoAr:

dx.doi.org/10.1021/om300182c | *Organometallics* 2012, 31, 3958−3971

(3)CoCl = 0.11:0.14:1.00. After 4 h, the ^{1}H NMR spectrum showed that there was no (3)Co(N_2) left, and the product ratio was now (3)CoH:(3)CoAr:(3)CoCl = 0.045:0.14:1. Assignments for (3)CoAr are based on analogy with previously reported (1)CoAr.

Tentative, partial assignments for (3)CoAr: ^{1}H NMR (benzene-d_6, 300 MHz): δ 10.27 (1H, t, J 7.6, Py *H4*), 5.14 (2H, d, J 7.1 Hz, CoAr *o*), −0.65 (6H, s, N=C*Me*). ^{19}F NMR (benzene-d_6, 282 MHz): δ −61.2.

(1)CoCH$_2$CMe$_2$Ph. Under an argon atmosphere, (1)$CoCl_2$ (0.32 g, 0.64 mmol) was weighed into a 50 mL Schlenk tube, followed by 12 mL of dry toluene. To the resulting green suspension, $ClMgCH_2CMe_2Ph$ (0.5 M in Et_2O, 0.80 mL) was added dropwise in around 30 min. The suspension turned pink. About 10 min later, another 0.85 mL of $ClMgCH_2CMe_2Ph$ solution was added over 30 min, and the suspension turned blue. After another 10 min, a final portion of 0.91 mL of the $ClMgCH_2CMe_2Ph$ solution was added dropwise (total amount of $ClMgCH_2CMe_2Ph$: 1.28 mmol). The resulting blue mixture was stirred for a further 1.5 h at room temperature. After evaporation of all solvents to dryness, 22 mL of dry toluene was added to dissolve most of the solid and the solution was filtered over Celite. The filtrate was concentrated to 2 mL and layered with hexane at −35 °C overnight. Pipetting off the mother liquor in the drybox left dark blue flakes of the product (0.16 g, 44%).

^{1}H NMR (benzene-d_6, 300 MHz): δ 10.82 (1H, t, J 7.4, Py *H4*), 7.79 (2H, d, J 7.4, Py *H3*), 7.45 (2H, t, J 7.4, NAr *p*), 7.29 (4H, d, J 8.0, NAr *m*), 6.99 (2H, t, J_{av} 7.3, Ph *m*), 6.91 (1H, t, J 6.8, Ph *p*), 6.63 (2H, d, J 7.4, Ph *o*), 2.02 (12H, s, NAr *o-Me*), 1.45 (2H, s, CoCH_2), 0.40 (6H, s, CMe_2), −1.93 (6H, s, N=C*Me*). ^{13}C NMR (benzene-d_6, 75 MHz): δ 167.0, 159.8, 158.8, 154.3, 130.4, 129.2 (NAr *m*), 127.5 (Ph *m*), 125.9 (NAr *p*), 125.0 (Ph *o*), 124.4 (Py *C3*), 123.6 (Ph *p*), 117.2 (Py *C4*), 47.3 (CMe_2), 31.6 (CMe_2), 26.0 (N=C*Me*), 19.6 (NAr *o-Me*), 0.9 (br, $CoCH_2$). Anal. Calcd for $C_{35}H_{40}CoN_3$ (561.65): C, 74.85; H, 7.18; N, 7.48. Found: C, 74.59; H, 7.17; N, 7.32.

(1)Co(η^3-allyl). Under an argon atmosphere, (1)$CoCl_2$ (0.58 g, 1.16 mmol) was weighed into a 50 mL Schlenk tube, followed by addition 20 mL of dry toluene. To the resulting green suspension was added 1.35 mL of allyl magnesium chloride solution (1.7 M in THF) in three portions (0.4 mL in 15 min; 0.80 mL in 1.5 h; 0.15 mL in 10 min). After the addition, the resulting orange mixture was stirred for 1.5 h at room temperature. After evaporation of all solvents, 24 mL of dry toluene was added to dissolve the solid, and the resulting suspension was filtered over Celite. The filtrated was concentrated and layered with hexane at −35 °C overnight. The mother liquor was pipetted off, leaving a dark orange solid (0.11 g, 20%).

^{1}H NMR (benzene-d_6, 300 MHz): δ 7.84 (2H, d, J 7.8, Py *H3*), 7.41 (1H, t, J 7.8, Py *H4*), 6.87−6.97 (6H, m, NAr *p* and *m*), 5.15 (1H, quintet, J 10.2, allyl C*H*), 2.42 (4H, br, allyl CH_2), 1.76 (12H, s, NAr *o-Me*), 1.55 (6H, s, N=C*Me*). ^{13}C NMR (benzene-d_6, 75 MHz): δ 150.1, 149.8, 149.2, 130.6, 128.3 (NAr *m*), 125.2 (NAr *p*), 120.5 (Py *C3*), 115.5 (Py *C4*), 106.1 (allyl CH), 43.9 (allyl CH_2), 18.5 (NAr o-*Me*), 16.6 (N=C*Me*). Anal. Calcd for $C_{28}H_{32}CoN_3$ (469.51): C, 71.63; H, 6.87; N, 8.95. Found: C, 71.75; H, 6.81; N, 8.82. Variable-temperature ^{1}H NMR spectra were recorded in toluene-d_8 (20 mg in 0.4 mL) over the range −60 to 70 °C; for an analysis of the dynamic behavior, see the SI. Low-temperature NMR data: ^{1}H NMR (toluene-d_8, 300 MHz, −60 °C): δ 7.84 (1H, d, J 7.8, Py *H3*), 7.51 (1H, d, J 7.6, Py *H5*), 7.41 (1H, t, J_{av} 7.7, Py *H4*), 6.87−6.97 (6H, m, NAr *p* and *m*), 5.24 (1H, tt, J 12.6 and 7.8, allyl C*H*), 3.40 (2H, br d, J 7.8, allyl H_{syn}), 1.57 (2H, br d, J 12.6, allyl H_{anti}), 1.85, 1.74 (6H each, s, NAr *o-Me*), 1.86, 1.21 (3H each, s, N=C*Me*).

(1)CoN=CH-4-C$_6$H$_4$Cl. In a N_2-filled drybox, (1)$CoCH_2SiMe_3$ (0.103 g, 0.20 mmol) was weighed in a small vial, followed by 4-chlorobenzonitrile (0.0278 g, 0.20 mmol). A 3 mL portion of dry toluene was added to dissolve the two reactants, and the resulting solution was transferred into a 25 mL Schlenk tube. A 20 mL amount of H_2 gas was injected into the stirred solution, and stirring of the resulting deep purple mixture was continued for 30 min. All solvents were evaporated to dryness. Then 3 mL of hexane and 0.5 mL of Et_2O were added, and the solution was cooled to −35 °C overnight. The dark crystalline product (0.096 g, 85%) was isolated by pipetting off the mother liquor and washing with dry hexane. One fragment of this crystalline material was used for determination of the crystal structure by single-crystal X-ray diffraction.

^{1}H NMR (benzene-d_6, 300 MHz): δ 9.62 (1H, s, N=C*H*), 7.92 (1H, t, J 7.7, Py *H4*), 7.63 (2H, d, J 7.7 Hz, Py *H3*), 7.01 (2H, d, J 8.3 Hz, NCAr *m*), 6.77 (2H, d, J 8.3 Hz, N=CAr *o*), 6.78−6.84 (6H, br, NAr *m,p*), 2.04 (s, 12H, NAr *o-Me*), 1.09 (s, 6H, N=C*Me*). ^{13}C NMR (benzene-d_6, 75 MHz): δ 156.7 (Py *C2*), 152.0 (NAr *i*), 148.6 (br, CoN=*C*), 147.5 (NC*Ar i*), 138.7 (NAr *o*), 132.9 (NCAr *p*), 130.0 (NCAr *m*), 127.6 (NAr *C-m*), 126.3 (NC*Ar C-o*), 124.9 (NAr C-*p*), 119.8 (Py *C3*), 115.6 (Py *C4*), 18.7 (NAr *o-Me*), 17.1 (N=C*Me*). N=CMe was not observed. Anal. Calcd for $C_{32}H_{32}ClCoN_4$ (567.01): C, 67.78; H, 5.69; N, 9.88. Found: C, 67.73; H, 5.45; N, 9.49.

General Procedure for the Reaction of (1)Co(N_2) with Organic Halides. In a drybox, (1)$CoCH_2SiMe_3$ (14 mg, 27 μmol) was weighed and dissolved in around 0.4 mL of benzene-d_6 in an NMR tube. Outside of the drybox, 2 mL of H_2 was injected into the tube; the solution turned green within one minute. The NMR tube was transferred back into the drybox, and the excess hydrogen was removed by flushing with nitrogen. The organic halide was then added: 1.0 equiv for aryl halides, 0.5 equiv for aliphatic halides. The NMR tube was vigorously shaken to mix the reactants. The reaction was monitored by ^{1}H NMR (and ^{19}F NMR where possible). The products were not isolated; attempted separations of (1)CoAr and (1)CoX were never successful. All reactions in Table 2 were done according to this procedure. For several (1)CoAr and (1)CoR complexes, ^{1}H NMR data were already provided in our previous communication.[11] Data for new compounds are provided below.

(1)Co(N_2) and Cyclopropylmethyl Chloride. The ^{1}H NMR spectrum recorded immediately after mixing showed that there was no (1)Co(N_2) left, but peaks were broad due to some suspended solids; the spectrum quality was much improved by first centrifuging the sample. Apart from a peak due to (1)CoCl, there were no triplets in the range 9.8−11 ppm, but there was a doublet at 7.9 ppm. By comparing to the ^{1}H NMR parameters of (1)Co(η^3-allyl), the new complex was identified as (1)Co(η^3-crotyl). In addition, a terminal olefin (probably 1-butene) could be observed. On the basis of the ^{1}H NMR data, the product ratio is (1)CoCl:(1)Co(η^3-crotyl):olefin:(cyclopropylmethyl chloride) = 1:0.55:0.25:0.12.

For (1)Co(η^3-crotyl): ^{1}H NMR (benzene-d_6, 300 MHz): δ 7.89 (2H, d, J 7.5, Py *H3*), 7.40 (1H, t, J 7.5, Py *H4*), 5.18 (1H, dt, J_d 11.2, J_t 9.2, CH_2CH), 2.48 (1H, dq, J_d 11.2, J_q 6.5, CH_3CH), 1.82 (2H, *, CH_2CH), 1.82 (12H, s, Ar *o*-Me), 1.57 (6H, s, N=C*Me*), 1.24 (3H, d, J 6.5, CH_3CH). Aryl hydrogens could not be unambiguously assigned.

(1)Co(N_2) and Allyl Chloride. The ^{1}H NMR spectrum of the purple solution, recorded immediately after mixing, showed that there was no (1)Co(N_2) left, but peaks were broad; quality improved after centrifugation. The spectrum showed (1)CoCl:(1)Co(η^3-allyl) = 1:0.98; no biallyl (1,5-hexadiene) could be detected.

(3)Co(N_2) and Allyl Chloride. The ^{1}H NMR spectrum of the purple solution showed the product ratio (3)CoCl:(3)Co(η^3-allyl) = 1:1, and no other products.

For (3)Co(η^3-allyl): ^{1}H NMR (benzene-d_6, 300 MHz): δ 7.82 (2H, d, J 7.4, Py *H3*), 5.11 (1H, quintet, J 10.2, allyl C*H*), 2.61−2.67 (4H, br d, allyl CH_2), 2.68−2.80 (4H, m, C*H*Me_2), 1.68 (6H, s, N=C*Me*), 1.19 (24H, br, CHMe_2). The pyridine H4 signal overlaps with the NAr peaks in the region 7.39−7.43 ppm. The remaining NAr peaks could not be unambiguously assigned.

(1)Co(N_2), (3)Co(N_2), and 6-Bromohexene. Analysis of these reaction mixtures was neither simple nor unambiguous, and we believe that chain walking and reversible β-elimination are the main causes of the observed complications. For a discussion, see the SI.

(1)Co(N_2) and Isobutyl Bromide. The ^{1}H NMR spectrum indicated formation of two (1)CoBr and (1)$CoCH_2CHMe_2$ (1:0.48). The alkyl complex decomposes slowly; after 24 h, the ratio is 1:0.33. Further separation of the two products was not tried.

For (1)$CoCH_2CHMe_2$: ^{1}H NMR (benzene-d_6, 300 MHz): δ 10.47 (1H, t, J 7.8, Py *H4*), 7.97 (2H, d, J 7.8, Py *H3*), 2.05 (12H, s, Ar *o*-Me), 1.64 (1H, m, C*H*Me_2), 0.86 (6H, d, CHMe_2), −1.75 (6H, s,

dx.doi.org/10.1021/om300182c | *Organometallics* 2012, 31, 3958−3971

N=C*Me*). Aryl hydrogen peaks and CoCH_2 cannot be unambiguously assigned

(1)Co(N_2) and Isopropyl Chloride. The ^{1}H NMR spectrum immediately after mixing (Figure S7) indicated the presence of three diamagnetic cobalt(I) complexes: (**1**)CoCl, (**1**)Co$CH_2CH_2CH_3$, and an unknown complex (Z) in the ratio 1:0.20:0.50. (**1**)Co$CH_2CH_2CH_3$ is not stable and decomposed over three days. However, unknown complex Z is stable.

For (**1**)Co$CH_2CH_2CH_3$: ^{1}H NMR (benzene-d_6, 300 MHz): δ 10.26 (1H, t, *J* 7.6, Py *H*4), 8.03 (2H, d, *J* 7.6, Py *H*3), 2.01 (12H, s, Ar *o*-Me), 1.14 (2H, t, Co$CH_2CH_2CH_3$), 0.35 (3H, t, *J* 7.0, $CoCH_2CH_2CH_3$), −1.14 (2H, m, $CoCH_2CH_2CH_3$), −1.61 (6H, s, N=C*Me*). Aryl hydrogen peaks and CoCH_2 could not be unambiguously assigned.

For complex Z: ^{1}H NMR (benzene-d_6, 300 MHz): δ 7.97 (1H, d, *J* 7.0), 7.44 (1H, d, *J* 5.5), 7.31 (1H, *), 2.14 (1H, *, C*H*Me_2), 2.11 (3H, s), 1.96 (3H, s), 1.85 (3H, s), 1.56 (3H, s), 1.16 (3H, d, *J* 7.0, CH*Me*$_2$), 0.99 (3H, d, *J* 6.6, CH*Me*$_2$), −0.81 (3H, s). A possible structure for this complex is proposed in the SI.

(1)Co(N_2) and *tert*-Butyl Iodide. The ^{1}H NMR spectrum immediately after mixing (Figure S8) showed four diamagnetic cobalt(I) complexes: (**1**)CoI, (**1**)CoCH_2CHMe_2, (^{t}Bu$_2$-**1**)CoI, and an unknown cobalt(I) complex (Z′), in the ratio 1:0.18:0.16:0.32. NMR data for (^{t}Bu$_2$-**1**)CoI are given below. For unknown complex Z′: ^{1}H NMR (benzene-d_6, 300 MHz): δ 8.02 (1H, d, *J* 7.0), 7.25 (*), −1.25 (3H, s).

(1)Co(N_2) and *tert*-Butyl Chloride. The reaction mixture turned purple after 5 min. The ^{1}H NMR spectrum of this solution showed the presence of (**1**)CoCl, (**1**)CoCH_2CHMe_2, and an unknown cobalt(I) complex most likely identical to Z′ obtained with *tert*-butyl iodide, in the ratio 1:0.08:0.32.

(1)Co(N_2) and 1-Iodoadamantane. The mixture turned pink immediately after mixing. The ^{1}H NMR spectrum indicated the generation of (**1**)CoI and an unknown cobalt(I) complex Z″ in the ratio 1:0.46. Complex Z″ appears to be similar but not identical to Z′ above. No obvious cobalt(I) alkyl could be observed.

For unknown complex Z″: ^{1}H NMR (benzene-d_6, 300 MHz): δ 7.99 (1H, d, *J* 6.2), 7.33 (*), −1.29 (3H, s).

(1)CoCl and Benzyl Chloride. In a N_2-filled drybox, (**1**)CoCl (14 mg, 29 μmol) was weighed and dissolved in about 0.4 mL of dry benzene-d_6. Benzyl chloride (3.4 μL, 29 μmol) was added. No obvious color change was observed, and the ^{1}H NMR spectrum immediately after mixing showed that no new product had been generated. After 10 min, solid started to precipitate. After 5 days at room temperature, the suspension was centrifuged. The ^{1}H NMR spectrum of the solution did not show any bibenzyl, while the ^{1}H NMR spectrum of the solid in CD_2Cl_2 showed it to be mainly (**1**)$CoCl_2$.

(1)CoCl and *p*-Trifuoromethylbenzyl Chloride. In a N_2-filled drybox, (**1**)CoCl (13 mg, 27 μmol) was weighed and dissolved in about 0.4 mL of dry benzene-d_6. *p*-Trifluoromethylbenzyl chloride (3.5 μL, 27 μmol) was added. No obvious color change was observed, and the ^{1}H NMR spectrum immediately after mixing showed that no new product had been generated. After 3 days at room temperature, a lot of dark solid had precipitated and the suspension was centrifuged. The ^{1}H NMR spectrum of the solution showed new singlets at 2.40 ppm (^{1}H) and −61.9 ppm (^{19}F) corresponding to 4,4′-trifluoromethylbibenzyl [$(CF_3C_6H_4CH_2)_2$:$CF_3C_6H_4CH_2Cl \approx$ 1:8; a few other fluorine-containing unidentified side products were also visible in the ^{19}F NMR]. After hydrolysis, analysis of the organic layer by GC/MS showed the presence of $(CF_3C_6H_4CH_2)_2$ and $CF_3C_6H_4CH_2Cl$ as well as a trace of $CF_3C_6H_4CH_3$.

(1)CoCl and Benzyl Bromide. In a N_2-filled drybox, (**1**)CoCl (14 mg, 29 μmol) was weighed and dissolved in about 0.4 mL of dry benzene-d_6. Benzyl bromide (3.5 μL, 29 μmol) was added. The resulting mixture turned green immediately and a lot of solid precipitated. After 10 min, the color turned purple. The ^{1}H NMR of this mixture showed that some benzyl bromide was left, but no (**1**)CoCl. After 5 days at room temperature, the mixture was red and contained suspended dark solid material. After centrifuging, the ^{1}H NMR of the liquid showed that bibenzyl had been generated, which was also confirmed by GC/MS. A spectrum of the solid in CD_2Cl_2 indicated the presence of a mixture of (**1**)$CoCl_2$, (**1**)CoClBr, and (**1**)$CoBr_2$.

General Procedure for C−C Coupling Reactions. To the product mixture of (**1**)CoAr and (**1**)CoX generated from (**1**)CoN_2 and ArX (1:1) as described earlier was added 0.5 equiv of the organic halide. For benzyl bromide and methyl iodide, the reaction was instantaneous; for benzyl chloride and allyl chloride it took hours for the reaction to complete. After addition of the alkyl halide, the mixture slowly turned green and deposited a dark solid. After the sample had turned gray, 0.5 mL of water was added. The organic layer was filtered over glass wool and examined by GC/MS. The results are shown in Table 3.

(1)Co(Py-6-Cl) and BzBr. When a mixture of (**1**)Co(Py-6-Cl) and (**1**)CoCl (1:1) generated from (**1**)Co(N_2) and 1.0 equiv of 2,6-dichloropyridine was reacted with 0.5 equiv of BzBr, a pink solution with dark suspended material was observed. After centrifugation, the pink supernatant solution was determined by NMR to be a mixture of cobalt(I) complexes (**1**)Co(Py-6-Cl):(**1**)CoBr:(**1**)CoCl = 1.0:0.67:0.44; the dark-colored solid was identified to be mainly (**1**)CoBrCl together with other DIP cobalt(II) dihalides. After addition of excess BzBr to the above pink solution, a cross-coupled product suspected to be 2-chloro-6-benzylpyridine could be detected by GC/MS.

(1)CoCH_2SiMe$_3$ and *tert*-Butyl Iodide. In a N_2-filled drybox, (**1**)CoCH_2SiMe$_3$ (70 mg, 136 μmol) was dissolved in 15 mL of dry toluene, and the resulting solution was transferred into a 25 mL Schlenk tube. Outside the drybox, 2-iodo-2-methylpropane (17 μL, 135 μmol) was injected into it. The resulting mixture was stirred at room temperature overnight, during which time a lot of solid precipitated. An additional 17 μL of 2-iodo-2-methylpropane was injected. After stirring at room temperature for another two days, the suspension was centrifuged and the liquid was evaporated to dryness. The resulting residue was dissolved in toluene and layered with pentane at −35 °C overnight. Some powder settled at the bottom; ^{1}H NMR showed that this consisted mainly of paramagnetic compound(s). The mother liquor was evaporated to dryness, and the residue dissolved in toluene. The resulting solution was allowed to slowly evaporate in a drybox at room temperature. After two days, some dark cubes of a crystalline solid were obtained. A fragment broken from one of these crystals was used in a single-crystal X-ray diffraction measurement. The data were of poor quality, and the attempted solution indicated that the crystal suffered from severe disorder and/or twinning problems. The structure *appeared* to correspond to (^{t}Bu$_2$-**1**)CoI, but even the connectivity cannot be considered to be definitive. Further details are given in the SI.

For (^{t}Bu$_2$-**1**)CoI: ^{1}H NMR (benzene-d_6, 300 MHz): δ 8.25 (1H, d, *J* 6.5, Py =C*H*), 7.80 (1H, t, *J* 7.3, Ar *p*), 7.45 (1H, d, *J* 7.3, Ar *m*), 7.31 (1H, d, *J* 7.3, Ar *m*), 6.60 (1H, t, *J* 7.4, Ar *p*), 6.51 (2H, d, *J* 7.4, Ar *m*), 3.23 (3H, s, N=C*Me*), 2.57 (3H, s, Ar *o*-Me), 2.44 (3H, s, Ar *o*-Me), 1.96 (3H, s, Ar *o*-Me), 1.84 (3H, s, Ar *o*-Me), 0.30 (9H, s, C*Me*$_3$), 0.27 (9H, s, C*Me*$_3$), −2.26 (1H, d, *J* 6.5, Py C*H*^{t}Bu), −2.79 (1H, s, Py C*H*^{t}Bu), −3.1 (3H, s, N=C*Me*). ^{13}C NMR (benzene-d_6, 75 MHz; from C−H HSQC spectrum): δ 128.2 (NAr *C*-*m*), 127.9 (NAr *m*), 127.6 (NAr *m*), 125.9 (NAr *p*), 125.3 (NAr *p*), 25.0 (C*Me*$_3$), 23.9(C*Me*$_3$), 20.7 (N=C*Me*), 19.6 (NAr *o*-*Me*), 19.2 (NAr *o*-*Me*), 18.5 (NAr *o*-Me), 18.3 (NAr *o*-*Me*).

Since neither (^{t}Bu$_2$-**1**)CoI nor (^{t}Bu$_2$-**1**)CoI_2 could be obtained pure, no elemental analysis was attempted.

(2)CoCH_2SiMe$_3$ and *tert*-Butyl Iodide. In a N_2-filled drybox, (**2**)CoCH_2SiMe$_3$ (100 mg, 175 μmol) was dissolved in 5 mL of dry toluene, and the resulting solution was transferred into a 25 mL Schlenk tube. Outside the drybox, 2-iodo-2-methylpropane (0.12 mL, 987 μmol, 5.6 equiv) was injected into it. After 10 min the mixture turned orange. It was stirred at room temperature overnight. After centrifuging, the liquid was evaporated to dryness. The residue was dissolved in dry toluene and layered with pentane at −35 °C overnight. Some oil together with some solids settled at the bottom. The liquid was pipetted off and evaporated to dryness. The residue was first washed with hexane, and then the residue was extracted by hexane/toluene (2:1). The resulting solution was cooled to −35 °C. After two days, the supernatant was pipetted off; the mother liquid and the solid were processed separately.

dx.doi.org/10.1021/om300182c | *Organometallics* 2012, 31, 3958−3971

Table 4. Details of Crystal Structure Determinations

	(**1**)CoN=CH-4-C_6H_4Cl	(**1**)Co(η^3-allyl)	(^{t}Bu$_2$-**2**)CoI (Cl)	(^{t}Bu$_2$-**2**)CoI$_2$
formula	$C_{32}H_{32}ClCoN_4$	$C_{28}H_{32}CoN_3$	$C_{37}H_{53}CoN_3I_{0.94}Cl_{0.06}$	$C_{37}H_{53}CoI_2N_3$
mol wt	567.00	469.50	720.17	852.55
T (K)	293(2)	293(2)	293(2)	200(2)
cryst syst	orthorhombic	orthorhombic	monoclinic	orthorhombic
space group	$P2_12_12_1$	$Pccn$	$P2_1/n$	$P2_12_12_1$
a/Å	10.9905(8)	19.1003(11)	13.586(5)	12.9841(8)
b/Å	14.5602(11)	30.6877(18)	16.687(7)	16.2444(10)
c/Å	18.7056(15)	8.3627(5)	16.630(6)	18.4949(11)
α/deg	90	90	90	90.00
β/deg	90	90	101.567(9)	90.00
γ/deg	90	90	90	90.00
V/Å^3	2993.3(4)	4901.7(5)	3694(2)	3900.9(4)
Z	4	8	4	4
D_c/g cm^{-3}	1.258	1.272	1.295	1.452
abs coeff/mm^{-1}	0.689	0.720	1.282	2.050
F_{000}	1184	1984	1495	1716
index ranges	$-13 \le h \le 13$	$-22 \le h \le 23$	$-16 \le h \le 16$	$-17 \le h \le 17$
	$-17 \le k \le 17$	$-37 \le k \le 37$	$-20 \le k \le 20$	$-20 \le k \le 21$
	$-22 \le l \le 22$	$-10 \le l \le 10$	$-20 \le l \le 20$	$-24 \le l \le 240$
$2\theta_{max}$/deg	51	51	51	56.68
no. reflns	19 632	27 619	26 916	71 802
no. unique	5568	4558	6870	9576
no. > 2σ	3614	2816	5955	8231
GOF	0.923	0.992	1.159	1.015
no. params	349	304	395	415
R ($F_o > 4\sigma(F)$)	0.0523	0.0435	0.0408	0.0344
R (all data)	0.0784	0.0930	0.0494	0.0445
wR_2 (all data)	0.1443	0.1444	0.1427	0.0979
largest peak, hole/e Å^{-3}	0.421, −0.350	0.363, −0.265	0.947, −0.765	1.472, −0.507

(a) The mother liquor was evaporated to dryness, and the residue dissolved in toluene. The resulting solution was allowed to slowly evaporate in a drybox at room temperature. After four days, some dark cubes of a crystalline solid were obtained. A fragment broken from one of these crystals was used for single-crystal X-ray diffraction, which showed it to be (^{t}Bu$_2$-**2**)CoI contaminated with about 6% of (^{t}Bu$_2$-**2**)CoCl.

(b) The ^{1}H NMR spectrum of the solid showed mainly diamagnetic (^{t}Bu$_2$-**2**)CoI (at least 70%) but also one or more paramagnetic compounds. The solid was washed with 0.2 mL of ether/hexane. The remaining solid was further extracted with ether (~0.5 mL)/toluene (6 drops), and the resulting solution was slowly evaporated to dryness over two weeks at room temperature to give a crystalline solid. A fragment broken off this solid was used for single-crystal X-ray diffraction, which showed it to be (^{t}Bu$_2$-**2**)CoI$_2$.

For (^{t}Bu$_2$-**2**)CoI: ^{1}H NMR (benzene-d_6, 300 MHz): δ 8.37 (1H, br d, Py =C*H*), 7.96 (1H, t, *J* 7.2, Ar *p*), 7.60 (1H, d, *J* 7.5, Ar *m*), 7.41 (1H, d, *J* 7.1, Ar *m*), 6.77 (1H, t, *J* 7.3, Ar *p*), 6.65 (2H, t, *J* 7.0, Ar *m*), 4.63 (1H, m, NAr C*H*$_2$CH$_3$), 3.46 (1H, m, NAr C*H*$_2$CH$_3$), 3.16 (1H, m, NAr C*H*$_2$CH$_3$), 2.73 (2H, m, NAr C*H*$_2$CH$_3$), 2.53 (1H, m, NAr C*H*$_2$CH$_3$), 2.21 (2H, m, NAr C*H*$_2$CH$_3$), 1.71 (t, 3H, J_{av} 7.4, NAr CH$_2$C*H*$_3$), 1.31 (t, 3H, J_{av} 7.4, NAr CH$_2$C*H*$_3$), 0.99 (t, 3H, J_{av} 7.4, NAr CH$_2$C*H*$_3$), 0.96 (t, 3H, J_{av} 7.5, NAr CH$_2$C*H*$_3$), 0.36 (s, 9H, C*Me*$_3$), 0.31 (s, 9H, C*Me*$_3$), −2.32 (1H, br d, Py C*H*^{t}Bu), −2.80 (1H, s, Py C*H*^{t}Bu), −3.01 (s, 3H, N=C*Me*).

For (^{t}Bu$_2$-**2**)CoI$_2$ (incomplete and tentative assignments; all peaks are broad): ^{1}H NMR (benzene-d_6, 300 MHz): δ 109.1 (1H, Py *H*3), 15.4 (9H, C*Me*$_3$), 12.2, 11.1, −16.1 (9H, C*Me*$_3$).

Since neither (^{t}Bu$_2$-**2**)CoI nor (^{t}Bu$_2$-**2**)CoI$_2$ could be obtained pure, no elemental analysis was attempted.

X-ray Structure Determinations. Crystal data and refinement parameters for the complexes are listed in Table 4. Details of individual structure determinations follow.

(1)CoN=CH-4-C_6H_4Cl. A deep purple fragment (approximately 0.20 × 0.20 × 0.25 mm) broken from a large crystal cluster was mounted in a thin glass capillary. Data were collected at 293 K in a Bruker four-circle diffractometer with an APEX detector using Mo Kα radiation (0.71073 Å). A sphere of data was collected with 0.2° scan width and 45 s scan time. The crystal system and space group were determined from the cell metrics and systematic absences. The data were integrated using the SAINT program,[39] and a semiempirical absorption correction was done using SADABS.[40] The structure was solved by Patterson methods using SHELXS[41] and refined using SHELXL97[41] (full-matrix least-squares refinement on F^2); hydrogen atoms were placed at calculated positions and refined in riding mode. The structure was checked for solvent-accessible voids with PLATON.[42]

(1)Co(η^3-allyl). A deep-orange crystal fragment (0.05 × 0.10 × 0.30 mm) was broken from a large piece of a crystalline aggregate and was sealed in a thin glass capillary and mounted on a Bruker D8 three-circle diffractometer equipped with a rotating anode generator (Mo Kα X-radiation), multilayer optics incident beam path, and an APEX-II CCD detector. A hemisphere of X-ray diffraction data (81 337 reflections) was collected to 60° 2θ using 25 s per 0.2° frame with a crystal-to-detector distance of 5 cm. A semiempirical absorption correction (SADABS) was applied, and identical data were merged to give 44 010 reflections covering the Ewald hemisphere, of which all data with up to 2θ = 51° were used for further refinement. The unit-cell parameters were obtained by least-squares refinement of 4833 reflections with $I > 10\sigma(I)$.

(^{t}Bu$_2$-1)CoI. For details of this (inconclusive) structure determination, see the SI.

(^{t}Bu$_2$-2)CoI (Cl). A deep-brown fragment (0.3 × 0.4 × 0.6 mm) was broken from a large piece of a crystalline aggregate and was sealed in a

dx.doi.org/10.1021/om300182c | *Organometallics* 2012, 31, 3958−3971

thin glass capillary and mounted on a Bruker D8 three-circle diffractometer equipped with a rotating anode generator (Mo Kα X-radiation), multilayer optics incident beam path, and an APEX-II CCD detector. A full sphere of X-ray diffraction data (132 039 reflections) was collected to $2\theta = 60°$ using 2 s per 0.3° frame with a crystal-to-detector distance of 5 cm. A semiempirical absorption correction (SADABS) was applied, and identical data were merged to give 42 999 reflections covering the Ewald hemisphere, of which all data up to $2\theta = 51°$ were used for further refinement. The unit-cell parameters were obtained by least-squares refinement of 9940 reflections with $I > 10\sigma(I)$. From the refinement results it became clear some (^{t}Bu$_2$-**2**)CoCl had cocrystallized with the (^{t}Bu$_2$-**2**)CoI (the Cl occupation refined to 6.3%). The source of this impurity is likely some (^{t}Bu$_2$-**2**)CoCl present in the starting material (^{t}Bu$_2$-**2**)CoCH$_2$SiMe$_3$.

(^{t}Bu$_2$-2)CoI$_2$. A deep purple crystal block (0.16 × 0.19 × 0.26 mm) broken from a large piece of crystal was selected under an inert atmosphere and mounted on a glass fiber. Unit cell measurements and intensity data collections were performed on a Bruker-AXS SMART 1K CCD diffractometer using graphite-monochromatized Mo Kα radiation (λ = 0.71073 Å). The measurement was done at 200 K. The data reduction included a correction for Lorentz and polarization effects, with an applied multiscan absorption correction (SADABS). The crystal structures were solved and refined using the SHELXTL program suite. Direct methods yielded all non-hydrogen atoms, which were refined with anisotropic thermal parameters. All hydrogen atom positions were calculated geometrically and were riding on their respective atoms. Thermal parameters of carbon atoms C26, C27, and C37 suggested the presence of positional disorder. Disorder for C26 and C27 was modeled as oscillation of the ethyl substituent moiety with partial occupancies of 50%:50%. Disorder for C37 was modeled as oscillation of the methyl end group of another ethyl substituent with partial occupancies of 50%:50%. A set of "rigid-bond" and "thermal parameters" restraints was applied to the disordered fragments to improve refinement of thermal parameters.

Computational Details. All geometries were optimized with Turbomole[43] using the TZVP basis set,[44] the b3-lyp functional,[45] and the unrestricted DFT formalism in combination with an external optimizer (PQS OPTIMIZE).[46] The low-spin state was found to be the lowest in energy for most species studied; square-planar Co(I) complexes preferred a broken-symmetry $S_z = 0$ solution.[20] Vibrational analyses were done to confirm the nature of all stationary points and to calculate thermal corrections (enthalpy and entropy, gas phase, 298 K, 1 bar) using the standard formulas of statistical thermodynamics. Improved single-point energies were obtained using the TZVPP basis set[47] at TZVP geometries and combined with TZVP-level thermal corrections to generate the final free energies.

■ ASSOCIATED CONTENT

Supporting Information

CIF file containing X-ray structure data for the structures determined in this work; total energies and *xyz* coordinate files for all optimized geometries. This material is available free of charge via the Internet at http://pubs.acs.org.

■ AUTHOR INFORMATION

Corresponding Author

*E-mail: Peter_Budzelaar@umanitoba.ca.

Notes

The authors declare no competing financial interest.

■ ACKNOWLEDGMENTS

We thank Mr. Mark Cooper (University of Manitoba) for help with X-ray structure determinations and Prof. Frank Hawthorne for the use of their single-crystal X-ray diffractometer. This work was supported by NSERC, CFI, and MRIF grants (to P.H.M.B.) and a University of Manitoba Graduate Fellowship and Manitoba Graduate Scholarship (to D.Z.).

■ REFERENCES

(1) (a) Johnson, L. K.; Killian, C. M.; Brookhart, M. *J. Am. Chem. Soc.* **1995**, *117*, 6414−6415. (b) Wissing, E.; Kaupp, M.; Boersma, J.; Spek, A. L.; Vankoten, G. *Organometallics* **1994**, *13*, 2349−2356. (c) Fedushkin, I. L.; Tishkina, A. N.; Fukin, G. K.; Hummert, M.; Schumann, H. *Eur. J. Inorg. Chem.* **2008**, 483−489. (d) Scarborough, C. C.; Wieghardt, K. *Inorg. Chem.* **2011**, *50*, 9773−9793.

(2) (a) Smith, A. L.; Clapp, L. A.; Hardcastle, K. I.; Soper, J. D. *Polyhedron* **2010**, *29*, 164−169. (b) Verma, P.; Weir, J.; Mirica, L.; Stack, T. D. P. *Inorg. Chem.* **2011**, *50*, 9816−9825.

(3) (a) Gibson, V. C.; Redshaw, C.; Solan, G. A. *Chem. Rev.* **2007**, *107*, 1745−1776. (b) Gibson, V. C.; Solan, G. A. Iron-based and Cobalt-based Polymerisation Catalysts. In *Metal Catalysts in Olefin Polymerization*; Guan, Z., Ed.; Springer: Berlin, 2009; Vol. *26*, pp 107−158.

(4) Chirik, P. J.; Wieghardt, K. *Science* **2010**, *327*, 794−795.

(5) Bart, S. C.; Lobkovsky, E. B.; Chirik, P. J. *Abstr. Pap. Am. Chem. Soc.* **2004**, *228*, U898−U898.

(6) Spessard, G. O.; Miessler, G. L. *Organometallic Chemistry*, 2nd ed.; Oxford University Press: Oxford, 2010.

(7) (a) Trovitch, R. J.; Lobkovsky, E.; Chirik, P. J. *J. Am. Chem. Soc.* **2008**, *130*, 11631−11640. (b) Trovitch, R. J.; Lobkovsky, E.; Bouwkamp, M. W.; Chirik, P. J. *Organometallics* **2008**, *27*, 6264−6278.

(8) (a) Doherty, J. C.; Ballem, K. H. D.; Patrick, B. O.; Smith, K. M. *Organometallics* **2004**, *23*, 1487−1489. (b) MacLeod, K. C.; Conway, J. L.; Tang, L. M.; Smith, J. J.; Corcoran, L. D.; Ballem, K. H. D.; Patrick, B. O.; Smith, K. M. *Organometallics* **2009**, *28*, 6798−6806.

(9) (a) Halpern, J.; Maher, J. P. *J. Am. Chem. Soc.* **1965**, *87*, 5361−5366. (b) Chock, P. B.; Halpern, J. *J. Am. Chem. Soc.* **1969**, *91*, 582−&. (c) Schneider, P. W.; Phelan, P. F.; Halpern, J. *J. Am. Chem. Soc.* **1969**, *91*, 77−. (d) Marzilli, L. G.; Marzilli, P. A.; Halpern, J. *J. Am. Chem. Soc.* **1971**, *93*, 1374−. (e) Halpern, J.; Phelan, P. F. *J. Am. Chem. Soc.* **1972**, *94*, 1881−1886.

(10) Ogoshi, H.; Setsune, J.; Yoshida, Z. *J. Am. Chem. Soc.* **1977**, *99*, 3869−3870.

(11) Zhu, D.; Budzelaar, P. H. M. *Organometallics* **2010**, *29*, 5759−5761.

(12) Smith, A. L.; Hardcastle, K. I.; Soper, J. D. *J. Am. Chem. Soc.* **2010**, *132*, 14358−14360.

(13) Enright, D.; Gambarotta, S.; Yap, G. P. A.; Budzelaar, P. H. M. *Angew. Chem., Int. Ed.* **2002**, *41*, 3873−3876.

(14) Zhu, D.; Thapa, I.; Korobkov, I.; Gambarotta, S.; Budzelaar, P. H. *Inorg. Chem.* **2011**, *50*, 9879−9887.

(15) (a) Cheung, C. W.; Chan, K. S. *Organometallics* **2011**, *30*, 4999−5009. (b) Cheung, C. W.; Chan, K. S. *Organometallics* **2011**, *30*, 4269−4283. (c) Cheung, C. W.; Chan, K. S. *Organometallics* **2011**, *30*, 1768−1771.

(16) Bowman, A. C.; Milsmann, C.; Atienza, C. C. H.; Lobkovsky, E.; Wieghardt, K.; Chirik, P. J. *J. Am. Chem. Soc.* **2010**, *132*, 1676−1684.

(17) (a) Knijnenburg, Q.; Horton, A. D.; van der Heijden, H.; Kooistra, T. M.; Hetterscheid, D. G. H.; Smits, J. M. M.; de Bruin, B.; Budzelaar, P. H. M.; Gal, A. W. *J. Mol. Catal. A: Chem.* **2005**, *232*, 151−159. (b) Tellmann, K. F.; Humphries, M. J.; Rzepa, H. S.; Gibson, V. C. *Organometallics* **2004**, *23*, 5503−5513.

(18) PhCH═CHPh and PhCH$_2$CH$_2$Ph detected by GC/MS after hydrolysis.

(19) (a) Erker, G.; Fromberg, W.; Atwood, J. L.; Hunter, W. E. *Angew. Chem., Int. Ed. Engl.* **1984**, *23*, 68−69. (b) Kaplan, A. W.; Polse, J. L.; Ball, G. E.; Andersen, R. A.; Bergman, R. G. *J. Am. Chem. Soc.* **1998**, *120*, 11649−11662. (c) Uhl, W.; Matar, M. *Z. Naturforsch. Sect. B: J. Chem. Sci.* **2004**, *59*, 1214−1222. (d) Temprado, M.; McDonough, J. E.; Mendiratta, A.; Tsai, Y. C.; Fortman, G. C.; Cummins, C. C.; Rybak-Akimova, E. V.; Hoff, C. D. *Inorg. Chem.* **2008**, *47*, 9380−9389.

(20) Knijnenburg, Q.; Hetterscheid, D.; Kooistra, T. M.; Budzelaar, P. H. M. *Eur. J. Inorg. Chem.* **2004**, 1204−1211.

(21) The (**3**)Co(N$_2$) used for this reaction was prepared via Na/Hg reduction of (**3**)CoCl$_2$.

(22) Note that since LCoAr and LCoX are formed in a ratio <1:1, "yields" of LCoX calculated from eq 1 may exceeed 100%.
(23) In our original communication[11] this product was incorrectly identified as (**1**)Co(2,4,6-^{t}Bu$_3$)C$_6$H$_2$.
(24) (a) Childress, B. C.; Rice, A. C.; Shevlin, P. B. *J. Org. Chem.* **1974**, *39*, 3056−3058. (b) Brunton, G.; Griller, D.; Barclay, L. R. C.; Ingold, K. U. *J. Am. Chem. Soc.* **1976**, *98*, 6803−6811.
(25) Bowry, V. W.; Lusztyk, J.; Ingold, K. U. *J. Am. Chem. Soc.* **1991**, *113*, 5687−5698.
(26) By contrast, 1-hexene was detected in the reaction between (**3**) Co(N$_2$) and 6-bromohexene. For details, refer to the Experimental Section.
(27) However, in that case one would expect a concentration dependence of the product ratio, which we did not observe. Further work is probably needed here.
(28) Bart, S. C.; Chlopek, K.; Bill, E.; Bouwkamp, M. W.; Lobkovsky, E.; Neese, F.; Wieghardt, K.; Chirik, P. J. *J. Am. Chem. Soc.* **2006**, *128*, 13901−13912.
(29) In the addition of most substrates *other* than vinyl acetate, the alkyl group is lost after the addition, forming a formally Fe(I) product, which in reality contains Fe(II) and a ligand radical anion.
(30) Reliable assignments of the paramagnetically shifted resonances were not possible; hence we do not know whether there is more than one paramagnetic component.
(31) Knijnenburg, Q.; Gambarotta, S.; Budzelaar, P. H. M. *Dalton Trans.* **2006**, 5442−5448.
(32) Reardon, D.; Conan, F.; Gambarotta, S.; Yap, G.; Wang, Q. Y. *J. Am. Chem. Soc.* **1999**, *121*, 9318−9325.
(33) Arrowsmith, M.; Hill, M. S.; Kociok-Kohn, G. *Organometallics* **2010**, *29*, 4203−4206.
(34) (a) Cahiez, G.; Moyeux, A. *Chem. Rev.* **2010**, *110*, 1435−1462. (b) Amatore, M.; Gosmini, C.; Perichon, J. *Eur. J. Org. Chem.* **2005**, 989−992.
(35) Fan, R. Q.; Zhu, D. S.; Mu, Y.; Li, G. H.; Yang, Y. L.; Su, Q.; Feng, S. H. *Eur. J. Inorg. Chem.* **2004**, 4891−4897.
(36) Schmidt, R.; Welch, M. B.; Knudsen, R. D.; Gottfried, S.; Alt, H. G. *J. Mol. Catal. A: Chem.* **2004**, *222*, 9−15.
(37) Zhu, D.; Janssen, F. F. B. J.; Budzelaar, P. H. M. *Organometallics* **2010**, *29*, 1897−1908.
(38) Kooistra, T. M.; Knijnenburg, Q.; Smits, J. M. M.; Horton, A. D.; Budzelaar, P. H. M.; Gal, A. W. *Angew. Chem., Int. Ed.* **2001**, *40*, 4719−+.
(39) *SMART* program suite, 6; Bruker AXS Inc: Madison, WI.
(40) Sheldrick, G. M. *SADABS*; University of Göttingen: Germany: 1996.
(41) Sheldrick, G. M. *Acta Crystallogr., Sect. A: Found. Crystallogr.* **2008**, *64*, 112−122.
(42) Spek, A. L. *PLATON. A Multipurpose Crystallographic Tool*; Utrecht University: Utrecht, The Netherlands, 2003.
(43) (a) Treutler, O.; Ahlrichs, R. *J. Chem. Phys.* **1995**, *102*, 346−354. (b) Ahlrichs, R.; Bär, M.; Baron, H.-P.; Bauernschmitt, R.; Böcker, S.; Ehrig, M.; Eichkorn, K.; Elliott, S.; Furche, F.; Haase, F.; Häser, M.; Hättig, C.; Horn, H.; Huber, C.; Huniar, U.; Kattannek, M.; Köhn, A.; Kölmel, C.; Kollwitz, M.; May, K.; Ochsenfeld, C.; Ohm, H.; Schäfer, A.; Schneider, U.; Treutler, O.; Tsereteli, K.; Unterreiner, B.; Von Arnim, M.; Weigend, F.; Weis, P.; Weiss, H. *Turbomole, 5*; Theoretical Chemistry Group, University of Karlsruhe, 2002.
(44) Schafer, A.; Huber, C.; Ahlrichs, R. *J. Chem. Phys.* **1994**, *100*, 5829−5835.
(45) (a) Lee, C. T.; Yang, W. T.; Parr, R. G. *Phys. Rev. B* **1988**, *37*, 785−789. (b) Becke, A. D. *J. Chem. Phys.* **1993**, *98*, 5648−5652. (c) Becke, A. D. *J. Chem. Phys.* **1993**, *98*, 1372−1377.
(46) (a) Baker, J. *J. Comput. Chem.* **1986**, *7*, 385−395. (b) Baker, J. *PQS, 2.4*; Parallel Quantum Solutions: Fayetteville, AR, 2001.
(47) Weigend, F.; Furche, F.; Ahlrichs, R. *J. Chem. Phys.* **2003**, *119*, 12753−12762.